

A Sparse Additive Model for High-Dimensional Interactions with an Exposure Variable

Sahir R Bhatnagar^{1,2}, Tianyuan Lu^{3,4}, Amanda Lovato⁵, David L Olds⁶,
Michael S Kobor⁷, Michael J Meaney⁸, Kieran O'Donnell⁹, Yi Yang¹⁰, and
Celia MT Greenwood^{1,3,5}

¹Department of Epidemiology, Biostatistics and Occupational Health,
McGill University

²Department of Diagnostic Radiology, McGill University

³Quantitative Life Sciences, McGill University

⁴Lady Davis Institute, Jewish General Hospital, Montréal, QC

⁵Statistics Canada, Ottawa, ON

⁶Department of Pediatrics, University of Colorado School of Medicine,
Denver

⁷Department of Medical Genetics, University of British Columbia, BC

⁸Singapore Institute for Clinical Sciences, Singapore; McGill University

⁹Department of Psychiatry, McGill University

¹⁰Department of Mathematics and Statistics, McGill University

¹¹Departments of Oncology and Human Genetics, McGill University

19

January 7, 2020

20

Abstract

21 A conceptual paradigm for onset of a new disease is often considered to be the
22 result of changes in entire biological networks whose states are affected by a complex
23 interaction of genetic and environmental factors. However, when modelling a relevant
24 phenotype as a function of high dimensional measurements, power to estimate inter-
25 actions is low, the number of possible interactions could be enormous and their effects
26 may be non-linear. Existing approaches for high dimensional modelling such as the
27 lasso might keep an interaction but remove a main effect, which is problematic for
28 interpretation. In this work, we introduce a method called **sail** for detecting non-
29 linear interactions with a key environmental or exposure variable in high-dimensional
30 settings which respects either the strong or weak heredity constraints. We prove that
31 asymptotically, our method possesses the oracle property, i.e., it performs as well as
32 if the true model were known in advance. We develop a computationally efficient
33 fitting algorithm with automatic tuning parameter selection, which scales to high-
34 dimensional datasets. Through an extensive simulation study, we show that **sail** out-
35 performs existing penalized regression methods in terms of prediction accuracy and
36 support recovery when there are non-linear interactions with an exposure variable.
37 We then apply **sail** to detect non-linear interactions between genes and a prenatal
38 psychosocial intervention program on cognitive performance in children at 4 years of
39 age. Results from our method show that individuals who are genetically predisposed
40 to lower educational attainment are those who stand to benefit the most from the
41 intervention. Our algorithms are implemented in an R package available on CRAN
42 (<https://cran.r-project.org/package=sail>).

1 INTRODUCTION

43 1 Introduction

44 Computational approaches to variable selection have become increasingly important with
45 the advent of high-throughput technologies in genomics and brain imaging studies, where
46 the data has become massive, yet where it is believed that the number of truly important
47 variables is small relative to the total number of variables. Although many approaches
48 have been developed for main effects, there is an enduring interest in powerful methods for
49 estimating interactions, since interactions may reflect important modulation of a genomic
50 system by an external factor and vice versa [2]. Accurate capture of interactions may hold the
51 potential to better understanding biological phenomena and improving prediction accuracy.
52 For example, a model that considered interactions between brain imaging data and genetic
53 features had better classification accuracy compared to a model that considered the main
54 effects only [24]. Furthermore, the manifestations of disease are often considered to be
55 the result of changes in entire biological networks whose states are affected by a complex
56 interaction of genetic and environmental factors [31]. However, there is a general deficit of
57 such replicated interactions in the literature [36]. Indeed, power to detect interactions is
58 always lower than for main effects, and in high-dimensional settings ($p \gg n$), this lack of
59 power to detect interactions is exacerbated, since the number of possible interactions could
60 be enormous and their effects may be non-linear. Hence, analytic methods that may improve
61 power are essential. Furthermore, methods capable of detecting non-linear interactions are
62 uncommon.

63 Interactions may occur in numerous types and of varying complexities. In this paper, we
64 consider one specific type of interaction model, where one exposure variable E is involved in
65 possibly non-linear interactions with a high-dimensional set of measures \mathbf{X} leading to effects
66 on a response variable, Y . We propose a multivariable penalization procedure for detecting
67 non-linear interactions between \mathbf{X} and E . Our method is motivated by the Nurse Family
68 Partnership (NFP); a program of prenatal and infancy home visiting by nurses for low-income

1 INTRODUCTION

mothers and their children [26]. In this intervention, NFP nurses guided pregnant women and parents of young children to improve the outcomes of pregnancy, their children's health and development, and their economic self-sufficiency, with the goal of reducing disparities over the life-course. Early intervention in young children has been shown to positively impact intellectual abilities [6], and more recent studies have shown that cognitive performance is also strongly influenced by genetic factors [30]. Given the important role of both environment and genetics, we are interested in finding interactions between these two components on cognitive function in children.

1.1 A sparse additive interaction model

Let $Y = (Y_1, \dots, Y_n) \in \mathbb{R}^n$ be a continuous outcome variable, $X_E = (E_1, \dots, E_n) \in \mathbb{R}^n$ a binary or continuous environment/exposure vector of known importance, and $\mathbf{X} = (X_1, \dots, X_p) \in \mathbb{R}^{n \times p}$ a matrix of additional predictors, possibly high-dimensional. Furthermore let $f_j : \mathbb{R} \rightarrow \mathbb{R}$ be a smoothing method for variable X_j by a projection on to a set of basis functions:

$$f_j(X_j) = \sum_{\ell=1}^{m_j} \psi_{j\ell}(X_j) \beta_{j\ell} \quad (1)$$

Here, the $\{\psi_{j\ell}\}_{\ell=1}^{m_j}$ are a family of basis functions in X_j [18]. Let Ψ_j be the $n \times m_j$ matrix of evaluations of the $\psi_{j\ell}$ and $\boldsymbol{\theta}_j = (\beta_{j1}, \dots, \beta_{jm_j}) \in \mathbb{R}^{m_j}$ for $j = 1, \dots, p$ ($\boldsymbol{\theta}_j$ is a m_j -dimensional column vector of basis coefficients for the j th main effect). In this article we consider an additive interaction regression model of the form

$$Y = \beta_0 \cdot \mathbf{1}_n + \sum_{j=1}^p \Psi_j \boldsymbol{\theta}_j + \beta_E X_E + \sum_{j=1}^p (X_E \circ \Psi_j) \boldsymbol{\tau}_j + \varepsilon \quad (2)$$

where $\beta_0 \in \mathbb{R}$ is the intercept, $\beta_E \in \mathbb{R}$ is the coefficient for the environment variable, $\boldsymbol{\tau}_j = (\tau_{j1}, \dots, \tau_{jm_j}) \in \mathbb{R}^{m_j}$ are the basis coefficients for the j th interaction term, $(X_E \circ \Psi_j)$ is the $n \times m_j$ matrix formed by the component-wise multiplication of the column vector X_E by

1 INTRODUCTION

85 each column of Ψ_j , and $\varepsilon \in \mathbb{R}^n$ is a vector of i.i.d errors with mean zero and finite variance.
86 Here we assume that p is large relative to n , and particularly that $\sum_{j=1}^p m_j/n$ is large. Due to
87 the large number of parameters to estimate with respect to the number of observations, one
88 commonly-used approach in the penalization literature is to shrink the regression coefficients
89 by placing a constraint on the values of $(\beta_E, \boldsymbol{\theta}_j, \boldsymbol{\tau}_j)$. Certain constraints have the added
90 benefit of producing a sparse model in the sense that many of the coefficients will be set
91 exactly to 0 [4]. Such a reduced predictor set can lead to a more interpretable model with
92 smaller prediction variance, albeit at the cost of having biased parameter estimates [12]. In
93 light of these goals, consider the following penalized objective function:

$$Q(\Phi) = -L(\Phi) + \lambda(1 - \alpha) \left(w_E |\beta_E| + \sum_{j=1}^p w_j \|\boldsymbol{\theta}_j\|_2 \right) + \lambda\alpha \sum_{j=1}^p w_{jE} \|\boldsymbol{\tau}_j\|_2 \quad (3)$$

94 where $\Phi = (\beta_0, \beta_E, \boldsymbol{\theta}_1, \dots, \boldsymbol{\theta}_p, \boldsymbol{\tau}_1, \dots, \boldsymbol{\tau}_p)$, $L(\Phi)$ is the log-likelihood function of the obser-
95 vations $\mathbf{V}_i = (Y_i, \Psi_i, X_{iE})$ for $i = 1, \dots, n$, $\|\boldsymbol{\theta}_j\|_2 = \sqrt{\sum_{k=1}^{m_j} \beta_{jk}^2}$, $\|\boldsymbol{\tau}_j\|_2 = \sqrt{\sum_{k=1}^{m_j} \tau_{jk}^2}$, $\lambda > 0$
96 and $\alpha \in (0, 1)$ are adjustable tuning parameters, w_E, w_j, w_{jE} are non-negative penalty fac-
97 tors for $j = 1, \dots, p$ which serve as a way of allowing parameters to be penalized differently.
98 The first term in the penalty penalizes the main effects while the second term penalizes the
99 interactions. The parameter α controls the relative weight on the two penalties. Note that
100 we do not penalize the intercept.

101 An issue with (3) is that since no constraint is placed on the structure of the model, it is
102 possible that an estimated interaction term is non-zero while the corresponding main effects
103 are zero. While there may be certain situations where this is plausible, statisticians have gen-
104 erally argued that interactions should only be included if the corresponding main effects are
105 also in the model [22]. This is known as the strong heredity principle [7]. Indeed, large main
106 effects are more likely to lead to detectable interactions [11]. In the next section we discuss
107 how a simple reparametrization of the model (3) can lead to this desirable property.

1 INTRODUCTION

108 1.2 Strong and weak heredity

109 The strong heredity principle states that an interaction term can only have a non-zero es-
 110 timate if its corresponding main effects are estimated to be non-zero, whereas the weak
 111 heredity principle allows for a non-zero interaction estimate as long as one of the corre-
 112 sponding main effects is estimated to be non-zero [7]. In the context of penalized regression
 113 methods, these principles can be formulated as structured sparsity [1] problems. Several
 114 authors have proposed to modify the type of penalty in order to achieve the heredity princi-
 115 ple [3, 17, 20, 28]. We take an alternative approach. Following Choi et al. [8], we introduce
 116 a new set of parameters $\boldsymbol{\gamma} = (\gamma_{1E}, \dots, \gamma_{pE}) \in \mathbb{R}^p$ and reparametrize the coefficients for the
 117 interaction terms $\boldsymbol{\tau}_j$ in (2) as a function of γ_{jE} and the main effect parameters $\boldsymbol{\theta}_j$ and β_E .
 118 This reparametrization for both strong and weak heredity is summarized in Table 1.

Table 1: Reparametrization for strong and weak heredity principle for **sail** model

Type	Feature	Reparametrization
Strong heredity	$\hat{\boldsymbol{\tau}}_j \neq 0$ only if $\hat{\boldsymbol{\theta}}_j \neq 0$ and $\hat{\beta}_E \neq 0$	$\boldsymbol{\tau}_j = \gamma_{jE}\beta_E\boldsymbol{\theta}_j$
Weak heredity	$\hat{\boldsymbol{\tau}}_j \neq 0$ only if $\hat{\boldsymbol{\theta}}_j \neq 0$ or $\hat{\beta}_E \neq 0$	$\boldsymbol{\tau}_j = \gamma_{jE}(\beta_E \cdot \mathbf{1}_{m_j} + \boldsymbol{\theta}_j)$

119 To perform variable selection in this new parametrization, we penalize $\boldsymbol{\gamma} = (\gamma_{1E}, \dots, \gamma_{pE})$
 120 instead of penalizing $\boldsymbol{\tau}$ as in (3), leading to the following penalized objective function:

$$Q(\boldsymbol{\Phi}) = -L(\boldsymbol{\Phi}) + \lambda(1 - \alpha) \left(w_E |\beta_E| + \sum_{j=1}^p w_j \|\boldsymbol{\theta}_j\|_2 \right) + \lambda\alpha \sum_{j=1}^p w_{jE} |\gamma_{jE}| \quad (4)$$

121 An estimate of the regression parameters is given by $\widehat{\boldsymbol{\Phi}} = \arg \min_{\boldsymbol{\Phi}} Q(\boldsymbol{\Phi})$. This penalty allows
 122 for the possibility of excluding the interaction term from the model even if the corresponding
 123 main effects are non-zero. Furthermore, smaller values for α would lead to more interactions
 124 being included in the final model while values approaching 1 would favor main effects. Similar
 125 to the elastic net [41], we fix α and obtain a solution path over a sequence of λ values.

1 INTRODUCTION

126 1.3 Toy example

127 We present here a toy example to better illustrate the methods proposed in this paper.
128 With a sample size of $n = 100$, we sample $p = 20$ covariates X_1, \dots, X_p independently from
129 a $N(0, 1)$ distribution truncated to the interval $[0, 1]$. Data were generated from a model
130 which follows the strong heredity principle, but where only one covariate, X_2 , is involved in
131 an interaction with a binary exposure variable, E :

$$Y = f_1(X_1) + f_2(X_2) + 1.75E + 1.5E \cdot f_2(X_2) + \varepsilon \quad (5)$$

132 For illustration, function $f_1(\cdot)$ is assumed to be linear, whereas function $f_2(\cdot)$ is non-linear:
133 $f_1(x) = -3x$, $f_2(x) = 2(2x - 1)^3$. The error term ε is generated from a normal distribution
134 with variance chosen such that the signal-to-noise ratio (SNR) is 2. We generated a single
135 simulated dataset and used the strong heredity **sail** method (described below) with cubic B-
136 splines to estimate the functional forms. 10-fold cross-validation (CV) was used to choose the
137 optimal value of penalization. We used $\alpha = 0.5$ and default values for all other arguments.
138 We plot the solution path for both main effects and interactions in Figure 1, coloring lines to
139 correspond to the selected model. We see that our method is able to correctly identify the true
140 model. We can also visually see the effect of the penalty and strong heredity principle working
141 in tandem, i.e., the interaction term $E \cdot f_2(X_2)$ (orange lines in the bottom panel) can only
142 be non-zero if the main effects E and $f_2(X_2)$ (black and orange lines respectively in the top
143 panel) are non-zero, while non-zero main effects does not imply a non-zero interaction.

1 INTRODUCTION

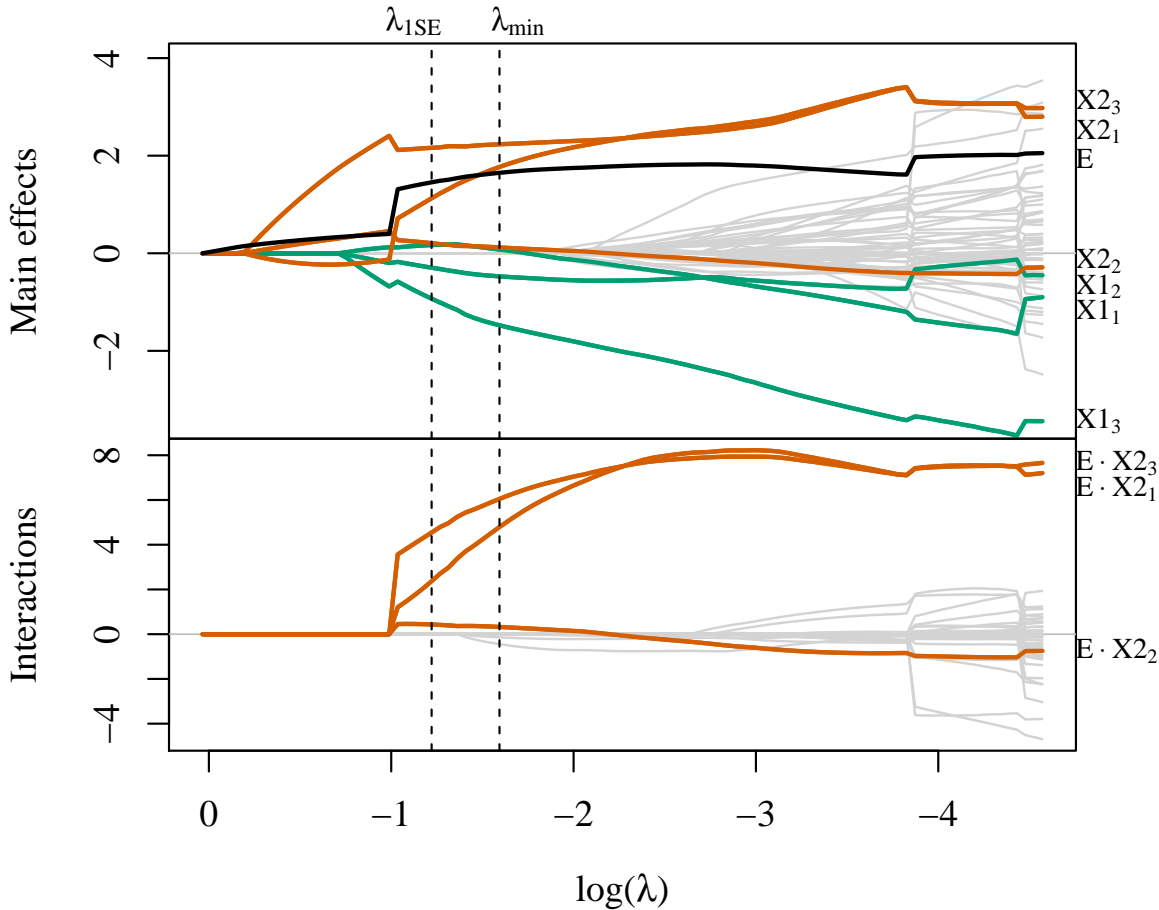


Figure 1: Toy example solution path for main effects (top) and interactions (bottom). $\{X_{11}, X_{12}, X_{13}\}$ and $\{X_{21}, X_{22}, X_{23}\}$ are the three basis coefficients for X_1 and X_2 , respectively. λ_{1SE} is the largest value of penalization for which the CV error is within one standard error of the minimizing value λ_{min} .

In Figure 2, we plot the true and estimated component functions $\hat{f}_1(X_1)$ and $E \cdot \hat{f}_2(X_2)$, and their estimates from this analysis with `sail`. We are able to capture the shape of the correct functional form, but the means are not well aligned with the data. Lack-of-fit for $f_1(X_1)$ can be partially explained by acknowledging that `sail` is trying to fit a cubic spline to a linear function. Nevertheless, this example demonstrates that `sail` can still identify trends reasonably well.

1 INTRODUCTION

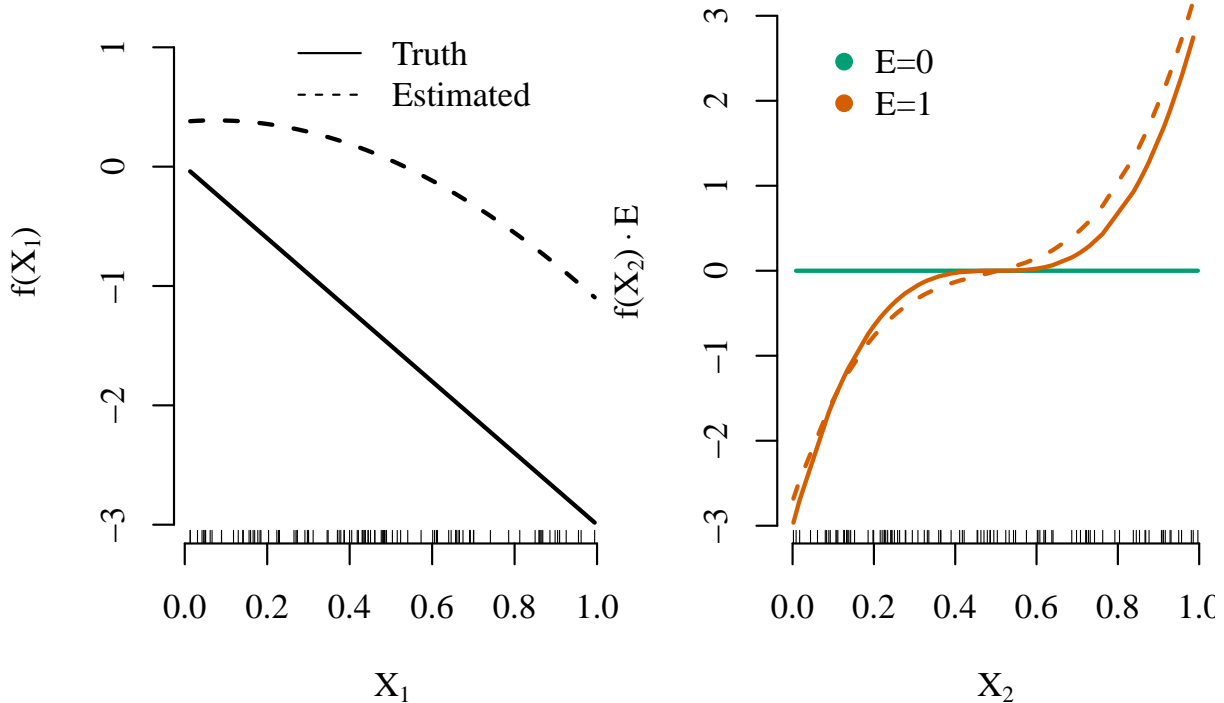


Figure 2: Estimated smooth functions for X_1 and the $X_2 \cdot E$ interaction by the **sail** method based on λ_{min} .

150 1.4 Related work

151 Methods for variable selection of interactions can be broken down into two categories: linear
152 and non-linear interaction effects. Many of the linear effect methods consider all pairwise
153 interactions in \mathbf{X} [3, 8, 33, 39] which can be computationally prohibitive when p is large.
154 More recent proposals for selection of interactions allow the user to restrict the search space
155 to interaction candidates [17, 20]. This is useful when the researcher wants to impose prior
156 information on the model. Two-stage procedures, where interaction candidates are con-
157 sidered from an original screen of main effects, have shown good performance when p is
158 large [15, 32] in the linear setting. There are many fewer methods available for estimating
159 non-linear interactions. For example, Radchenko and James (2010) [28] proposed a model

1 INTRODUCTION

160 of the form

$$Y = \beta_0 + \sum_{j=1}^p f_j(X_j) + \sum_{j>k} f_{jk}(X_j, X_k) + \varepsilon$$

161 where $f(\cdot)$ are smooth component functions. This method is more computationally expensive
162 than **sail** since it considers all pairwise interactions between the basis functions, and its
163 effectiveness in simulations or real-data applications is unknown as there is no software
164 implementation.

165 While working on this paper, we were made aware of the recently proposed pliable lasso [35]
166 which considers the interactions between $\mathbf{X}_{n \times p}$ and another matrix $\mathbf{Z}_{n \times K}$ and takes the
167 form

$$Y = \beta_0 + \sum_{j=1}^p \beta_j X_j + \sum_{j=1}^K \theta_j Z_j + \sum_{j=1}^p (X_j \circ \mathbf{Z}) \boldsymbol{\alpha}_j + \varepsilon \quad (6)$$

168 where $\boldsymbol{\alpha}_j$ is a K -dimensional vector. Our proposal is most closely related to this method
169 with \mathbf{Z} being a single column matrix; the key difference being the non-linearity effects of our
170 predictor variables. As pointed out by the authors of the pliable lasso, either their method
171 or ours can be seen as a varying coefficient model, i.e., the effect of X varies as a function
172 of the exposure variable E or \mathbf{Z} in (6).

173 The main contributions of this paper are five-fold. First, we develop a model for non-
174 linear interactions with a key exposure variable, following either the weak or strong hered-
175 ity principle, that is computationally efficient and scales to the high-dimensional setting
176 ($n \ll p$). Second, through simulation studies, we show improved performance in terms of
177 prediction accuracy and support recovery over existing methods that only consider linear
178 interactions or additive main effects. Third, we show that our method possesses the oracle
179 property [13], i.e., it performs as well as if the true model were known in advance. Fourth,
180 we demonstrate the performance of our method in two applications: 1) gene-environment
181 interactions in a prenatal psychosocial intervention program [26] and 2) a study aimed at
182 identifying which clinical variables influence mortality rates amongst seriously ill hospital-

2 COMPUTATION

183 sized patients [10]. Fifth, we implement our algorithms in the **sail** R package on CRAN
184 (<https://cran.r-project.org/package=sail>), along with extensive documentation. In
185 particular, our implementation also allows for linear interaction models, user-defined basis
186 expansions, a cross-validation procedure for selecting the optimal tuning parameter, and
187 differential shrinkage parameters to apply the adaptive lasso idea [40].

188 The rest of the paper is organized as follows. Section 2 describes our optimization procedure
189 and some details about the algorithm used to fit the **sail** model for the least squares case.
190 Theoretical results are given in Section 3. In Section 4, through simulation studies we
191 compare the performance of our proposed approach and demonstrate the scenarios where it
192 can be advantageous to use **sail** over existing methods. Section 5 contains two real data
193 examples and Section 6 discusses some limitations and future directions.

194 2 Computation

195 In this section we describe a blockwise coordinate descent algorithm for fitting the least-
196 squares version of the **sail** model in (4). We fix the value for α and minimize the objective
197 function over a decreasing sequence of λ values ($\lambda_{max} > \dots > \lambda_{min}$). We use the subgradi-
198 ent equations to determine the maximal value λ_{max} such that all estimates are zero. Due
199 to the heredity principle, this reduces to finding the largest λ such that all main effects
200 $(\beta_E, \boldsymbol{\theta}_1, \dots, \boldsymbol{\theta}_p)$ are zero. Following Friedman et al. [14], we construct a λ -sequence of 100
201 values decreasing from λ_{max} to $0.001\lambda_{max}$ on the log scale, and use the warm start strategy
202 where the solution for λ_ℓ is used as a starting value for $\lambda_{\ell+1}$.

2 COMPUTATION

203 2.1 Blockwise coordinate descent for least-squares loss

204 The strong heredity **sail** model with least-squares loss has the form

$$\hat{Y} = \beta_0 \cdot \mathbf{1} + \sum_{j=1}^p \Psi_j \boldsymbol{\theta}_j + \beta_E X_E + \sum_{j=1}^p \gamma_{jE} \beta_E (X_E \circ \Psi_j) \boldsymbol{\theta}_j \quad (7)$$

205 and the objective function is given by

$$Q(\Phi) = \frac{1}{2n} \left\| Y - \hat{Y} \right\|_2^2 + \lambda(1 - \alpha) \left(w_E |\beta_E| + \sum_{j=1}^p w_j \|\boldsymbol{\theta}_j\|_2 \right) + \lambda \alpha \sum_{j=1}^p w_{jE} |\gamma_{jE}| \quad (8)$$

206 Solving (8) in a blockwise manner allows us to leverage computationally fast algorithms for
207 ℓ_1 and ℓ_2 norm penalized regression. We show in Supplemental Section B that by careful
208 construction of pseudo responses and pseudo design matrices, existing efficient algorithms can
209 be used to estimate the parameters. Indeed, the objective function simplifies to a modified
210 lasso problem when holding all $\boldsymbol{\theta}_j$ fixed, and a modified group lasso problem when holding
211 β_E and all γ_{jE} fixed. We provide an overview of the computations in Algorithm 1.

212 2.2 Weak Heredity

213 Our method can be easily adapted to enforce the weak heredity property. That is, an
214 interaction term can only be present if at least one of its corresponding main effects is
215 non-zero. To do so, we reparametrize the coefficients for the interaction terms in (2) as
216 $\boldsymbol{\alpha}_j = \gamma_{jE} (\beta_E \cdot \mathbf{1}_{m_j} + \boldsymbol{\theta}_j)$, where $\mathbf{1}_{m_j}$ is a vector of ones with dimension m_j (i.e. the length of $\boldsymbol{\theta}_j$).
217 We defer the algorithm details for fitting the **sail** model with weak heredity in Supplemental
218 Section B.4, as it is very similar to Algorithm 1 for the strong heredity **sail** model.

2 COMPUTATION

Algorithm 1 Blockwise Coordinate Descent for Least-Squares **sail** with Strong Heredity.

For a decreasing sequence $\lambda = \lambda_{max}, \dots, \lambda_{min}$ and fixed α :

1. Initialize $\beta_0^{(0)}, \beta_E^{(0)}, \boldsymbol{\theta}_j^{(0)}, \gamma_{jE}^{(0)}$ for $j = 1, \dots, p$ and set iteration counter $k \leftarrow 0$.
 2. Repeat the following until convergence:
 - (a) update $\boldsymbol{\gamma} = (\gamma_{1E}, \dots, \gamma_{pE})$
 - i. Compute the pseudo design: $\tilde{X}_j \leftarrow \beta_E^{(k)}(X_E \circ \boldsymbol{\Psi}_j)\boldsymbol{\theta}_j^{(k)}$ for $j = 1, \dots, p$
 - ii. Compute the pseudo response \tilde{Y} by removing the contribution of every term not involving $\boldsymbol{\gamma}$ from Y
 - iii. Solve:

$$\boldsymbol{\gamma}^{(k)(new)} \leftarrow \arg \min_{\boldsymbol{\gamma}} \frac{1}{2n} \left\| \tilde{Y} - \sum_j \gamma_{jE} \tilde{X}_j \right\|_2^2 + \lambda \alpha \sum_j w_{jE} |\gamma_{jE}| \quad (9)$$
 - iv. Set $\boldsymbol{\gamma}^{(k)} = \boldsymbol{\gamma}^{(k)(new)}$
 - (b) update $\boldsymbol{\theta} = (\boldsymbol{\theta}_1, \dots, \boldsymbol{\theta}_p)$
 - for $j = 1, \dots, p$
 - i. Compute the pseudo design: $\tilde{X}_j \leftarrow \boldsymbol{\Psi}_j + \gamma_{jE}^{(k)} \beta_E^{(k)}(X_E \circ \boldsymbol{\Psi}_j)$
 - ii. Compute the pseudo response (\tilde{Y}) by removing the contribution of every term not involving $\boldsymbol{\theta}_j$ from Y
 - iii. Solve:

$$\boldsymbol{\theta}_j^{(k)(new)} \leftarrow \arg \min_{\boldsymbol{\theta}_j} \frac{1}{2n} \left\| \tilde{Y} - \tilde{X}_j \boldsymbol{\theta}_j \right\|_2^2 + \lambda(1 - \alpha) w_j \|\boldsymbol{\theta}_j\|_2 \quad (10)$$
 - iv. Set $\boldsymbol{\theta}_j^{(k)} \leftarrow \boldsymbol{\theta}_j^{(k)(new)}$
 - (c) update β_E
 - i. Compute the pseudo design: $\tilde{X}_E \leftarrow X_E + \sum_j \gamma_{jE}^{(k)}(X_E \circ \boldsymbol{\Psi}_j)\boldsymbol{\theta}_j^{(k)}$
 - ii. Compute the pseudo response (\tilde{Y}) by removing the contribution of every term not involving β_E from Y
 - iii. Soft-threshold update ($S(x, t) = \text{sign}(x)(|x| - t)_+$):

$$\beta_E^{(k)(new)} \leftarrow \frac{1}{\tilde{X}_E^\top \tilde{X}_E} S \left(\frac{1}{n \cdot w_E} \tilde{X}_E^\top \tilde{Y}, \lambda(1 - \alpha) \right) \quad (11)$$
 - iv. Set $\beta_E^{(k+1)} \leftarrow \beta_E^{(k)(new)}$, $k \leftarrow k + 1$
-

2 COMPUTATION

219 2.3 Adaptive sail

220 The weights for the environment variable, main effects and interactions are given by w_E, w_j
221 and w_{jE} respectively. These weights serve as a means of allowing a different penalty to be
222 applied to each variable. In particular, any variable with a weight of zero is not penalized
223 at all. This feature is usually selected for one of two reasons:

- 224 1. Prior knowledge about the importance of certain variables is known. Larger weights
225 will penalize the variable more, while smaller weights will penalize the variable less

226 2. Allows users to apply the adaptive **sail**, similar to the adaptive lasso [40]

227 We describe the adaptive **sail** in Algorithm 2. This is a general procedure that can be
228 applied to the weak and strong heredity settings, as well as both least squares and logistic
229 loss functions. We provide this capability in the **sail** package using the **penalty.factor**
230 argument and provide an example in Supplemental Section ??.

Algorithm 2 Adaptive **sail** algorithm

1. For a decreasing sequence $\lambda = \lambda_{max}, \dots, \lambda_{min}$ and fixed α run the **sail** algorithm
 2. Use cross-validation or a data splitting procedure to determine the optimal value for the tuning parameter: $\lambda^{[opt]} \in \{\lambda_{max}, \dots, \lambda_{min}\}$
 3. Let $\widehat{\beta}_E^{[opt]}, \widehat{\theta}_j^{[opt]}$ and $\widehat{\tau}_j^{[opt]}$ for $j = 1, \dots, p$ be the coefficient estimates corresponding to the model at $\lambda^{[opt]}$
 4. Set the weights to be
$$w_E = \left(\left| \widehat{\beta}_E^{[opt]} \right| + 1/n \right)^{-1}, w_j = \left(\|\widehat{\theta}_j^{[opt]}\|_2 + 1/n \right)^{-1}, w_{jE} = \left(\|\widehat{\tau}_j^{[opt]}\|_2 + 1/n \right)^{-1}$$
for $j = 1, \dots, p$
 5. Run the **sail** algorithm with the weights defined in step 4), and use cross-validation or a data splitting procedure to choose the optimal value of λ
-

231 2.4 Flexible design matrix

232 The definition of the basis expansion functions in (1) is very flexible, in the sense that our
233 algorithms are independent of this choice. As a result, the user can apply any basis expansion
234 they desire. In the extreme case, one could apply the identity map, i.e., $f_j(X_j) = X_j$ which

3 THEORY

leads to a linear interaction model (referred to as `linear sail`). When little information is known a priori about the relationship between the predictors and the response, by default, we choose to apply the same basis expansion to all columns of \mathbf{X} . This is a reasonable approach when all the variables are continuous. However, there are often situations when the data contains a combination of categorical and continuous variables. In these cases it may be sub-optimal to apply a basis expansion to the categorical variables. Owing to the flexible nature of our algorithm, we can handle this scenario in our implementation by allowing a user-defined design matrix. The only extra information needed is the group membership of each column in the design matrix. We illustrate such an example in a vignette of the `sail R` package.

3 Theory

In this section we study the asymptotic behaviour of the `sail` estimator $\widehat{\Phi}$, defined as the minimizer of (4), as well as the model selection properties. We show that `sail` possesses the oracle property when the sample size approaches infinity and the number of predictors is fixed. That is, under certain regularity conditions, it performs as well as if the true model were known in advance and has the optimal estimation rate [40]. The regularity conditions and proofs are given in Supplemental Section A.

Let $\Phi^* = (\beta_E^*, \boldsymbol{\theta}_1^{*\top}, \dots, \boldsymbol{\theta}_p^{*\top}, \gamma_{1E}^*, \dots, \gamma_{pE}^*)^\top$ denote the unknown vector of true coefficients in (4). To simplify the notation, we use the representation $\Phi^* = (\boldsymbol{\phi}_1^{*\top}, \boldsymbol{\phi}_2^{*\top}, \dots, \boldsymbol{\phi}_{p+1}^{*\top}, \boldsymbol{\phi}_{p+2}^{*\top}, \dots, \boldsymbol{\phi}_{2p+1}^{*\top})^\top$, where $\boldsymbol{\phi}_1^* = \beta_E^*$, $\boldsymbol{\phi}_2^* = \boldsymbol{\theta}_1^*, \dots, \boldsymbol{\phi}_{p+1}^* = \boldsymbol{\theta}_p^*$, and $\boldsymbol{\phi}_{p+2}^* = \gamma_{1E}^*, \dots, \boldsymbol{\phi}_{2p+1}^* = \gamma_{pE}^*$. Denote by $\mathcal{A} = \{m : \boldsymbol{\phi}_m^* \neq \mathbf{0}\}$ the unknown sparsity pattern of Φ^* , and $\widehat{\mathcal{A}} = \left\{m : \widehat{\boldsymbol{\phi}}_m \neq \mathbf{0}\right\}$ the estimated `sail` model selector. We can rewrite the penalty terms in (4), and consider the

3 THEORY

257 sail estimates $\widehat{\Phi}_n$ given b

$$\widehat{\Phi}_n = \arg \min_{\Phi} Q_n(\Phi) = -L_n(\Phi) + n\lambda_m \sum_{m=1}^{2p+1} \|\phi_m\|_2, \quad (12)$$

258 where $\lambda_1 = \lambda(1 - \alpha)w_E$, $\lambda_m = \lambda(1 - \alpha)w_m$ for $m = 2, \dots, p + 1$, and $\lambda_m = \lambda\alpha w_{mE}$ for
259 $m = p + 2, \dots, 2p + 1$. Define

$$\mathcal{A}_1 = \{m : \phi_m^* \neq \mathbf{0} \ (1 \leq m \leq p+1)\}, \quad \mathcal{A}_2 = \{m : \phi_m^* \neq \mathbf{0} \ (p+2 \leq m \leq 2p+1)\}, \quad \mathcal{A} = \mathcal{A}_1 \cup \mathcal{A}_2$$

260 that is, \mathcal{A}_1 contains the indices for main effects whose true coefficients are non-zero, and \mathcal{A}_2
261 contains the indices for interaction terms whose true coefficients are non-zero. Let

$$a_n = \max \{\lambda_m, \lambda_{m'} : m \in \mathcal{A}_1, m' \in \mathcal{A}_2\}$$

262

$$b_n = \min \{\lambda_m, \lambda_{m'} : m \in \mathcal{A}_1^c, m' \in \mathcal{A}_2^c \text{ s.t. } \phi_{m'}^* = \gamma_{jE}^* = 0 \text{ but } \beta_E \neq 0 \text{ and } \theta_j^* \neq \mathbf{0} \quad (1 \leq j \leq p)\}$$

263 Note that our asymptotic results are stated for the main effects and interaction terms only,
264 even though our formulation includes an unpenalized intercept. Consistency results imme-
265 diately follow for β_0 since we assume the data has been centered, leading to a closed form
266 solution for the intercept in the least-squares setting.

267 **Lemma 1.** [Existence of a local minimizer] If $a_n = o(\frac{1}{\sqrt{n}})$ as $n \rightarrow \infty$, i.e. $\sqrt{n}a_n \rightarrow 0$, then

$$268 \quad \|\widehat{\Phi}_n - \Phi^*\|_2 = O_p(\frac{1}{\sqrt{n}})$$

269 Lemma (1) states that if the tuning parameters corresponding to the non-zero coefficients
270 converge to 0 at a speed faster than $\frac{1}{\sqrt{n}}$, then there exists a local minimizer of $Q_n(\Phi)$ which
271 is \sqrt{n} -consistent [8, 37].

272 **Theorem 1** (Model selection consistency). If $\sqrt{n}a_n \rightarrow 0$ and $\sqrt{n}b_n \rightarrow \infty$, then

$$P \left(\widehat{\Phi}_{\mathcal{A}_1^c} = \mathbf{0} \right) \rightarrow 1 \quad \text{and} \quad P \left(\widehat{\Phi}_{\mathcal{A}_2^c} = \mathbf{0} \right) \rightarrow 1 \quad (13)$$

3 THEORY

273 Theorem (1) shows that `sail` can consistently remove the main effects and interaction terms
274 which are not associated with the response with high probability. Together with Lemma (1),
275 we see that the asymptotic behaviour of the penalty terms for the zero and non-zero predic-
276 tors must be different to satisfy the model selection consistency property (13) [23]. Specif-
277 ically, when the tuning parameters for the non-zero coefficients converge to 0 faster than
278 $1/\sqrt{n}$ (i.e. $\sqrt{n}a_n \rightarrow 0$) and those for zero coefficients are large enough (i.e. $\sqrt{nb_n} \rightarrow$
279 ∞), the Lemma (1) and Theorem (1) imply that the \sqrt{n} -consistent estimator $\widehat{\Phi}_n$ satisfies
280 $P(\widehat{\Phi}_{\mathcal{A}_2^c} = \mathbf{0}) \rightarrow 1$.

281 Next, we obtain the asymptotic distribution of the `sail` estimator.

282 **Theorem 2** (Asymptotic normality). *Denote $\mathcal{A} = \mathcal{A}_1 \cup \mathcal{A}_2$. Assume that $\sqrt{n}a_n \rightarrow 0$ and
283 $\sqrt{nb_n} \rightarrow \infty$. Under the regularity conditions, the subvector $\widehat{\Phi}_{\mathcal{A}}$ of the local minimizer $\widehat{\Phi}_n$
284 given in Lemma (1) satisfies*

$$\sqrt{n} (\widehat{\Phi}_{\mathcal{A}} - \Phi_{\mathcal{A}}^*) \xrightarrow{d} N(\mathbf{0}, \mathbf{I}^{-1}(\Phi_{\mathcal{A}}^*)) , \quad (14)$$

285 where $\mathbf{I}(\Phi_{\mathcal{A}}^*)$ is the Fisher information matrix for $\Phi_{\mathcal{A}}$ at $\Phi_{\mathcal{A}} = \Phi_{\mathcal{A}}^*$, assuming \mathcal{A}_c is known
286 in advance.

287 Together, Theorems (1) and (2) establish that if the tuning parameters satisfy the conditions
288 $\sqrt{n}a_n \rightarrow 0$ and $\sqrt{nb_n} \rightarrow \infty$, then as the sample size grows large, `sail` has the oracle
289 property [13]. In order for the conditions on the tuning parameters to be satisfied, we follow
290 the strategies outlined for the adaptive Lasso [40], the adaptive group Lasso [23] and the
291 adaptive elastic-net [42]. That is, we define the adaptive weights as $w_m = \|\widehat{\phi}_m^{\text{init}} + 1/n\|_2^{-\xi}$
292 for $m = 1, \dots, 2p + 1$, where ξ is a positive constant and $\widehat{\phi}_m^{\text{init}}$ is an initial \sqrt{n} -consistent
293 estimate of ϕ_m^* . Here, the $1/n$ is to avoid division by zero.

4 SIMULATION STUDY

294 4 Simulation Study

295 In this section, we use simulated data to understand the performance of `sail` in different
296 scenarios.

297 4.1 Comparator Methods

298 Since there are no other packages that directly address our chosen problem, we selected
299 comparator methods based on the following criteria: 1) penalized regression methods that
300 can handle high-dimensional data ($n < p$), 2) allowing at least one of linear effects, non-
301 linear effects or interaction effects, and 3) having a software implementation in R. The selected
302 methods can be grouped into three categories:

- 303 1. Linear main effects: `lasso` [34], `adaptive lasso` [40]
- 304 2. Linear interactions: `lassoBT` [32], `GLinternet` [20]
- 305 3. Non-linear main effects: `HierBasis` [16], `SPAM` [29], `gamsel` [9]

306 For `GLinternet` we specified the `interactionCandidates` argument so as to only consider
307 interactions between the environment and all other X variables. For all other methods we
308 supplied (\mathbf{X}, X_E) as the data matrix, 100 for the number of tuning parameters to fit, and
309 used the default values otherwise¹. `lassoBT` considers all pairwise interactions as there is
310 no way for the user to restrict the search space. `SPAM` applies the same basis expansion to
311 every column of the data matrix; we chose 5 basis spline functions. `HierBasis` and `gamsel`
312 selects whether a term in an additive model is non-zero, linear, or a non-linear spline up to
313 a specified max degrees of freedom per variable.

314 We compare the above listed methods with our main proposal method `sail`, as well as
315 with `adaptive sail` (Algorithm 2) and `sail weak` which has the weak heredity property.

¹R code for each method available at https://github.com/sahirbhatnagar/sail/blob/master/my_sims/method_functions.R

4 SIMULATION STUDY

316 For each function f_j , we use a B-spline basis matrix with `degree=5` implemented in the `bs`
317 function in R [27]. We center the environment variable and the basis functions before running
318 the `sail` method.

319 4.2 Simulation Design

320 To make the comparisons with other methods as fair as possible, we followed a simulation
321 framework that has been previously used for variable selection methods in additive mod-
322 els [19, 21]. We extend this framework to include interaction effects as well. The covariates
323 are simulated as follows. First, we generate x_1, \dots, x_{1000} independently from a standard nor-
324 mal distribution truncated to the interval $[0,1]$ for $i = 1, \dots, n$. The first four variables are
325 non-zero (i.e. active in the response), while the rest of the variables are zero (i.e. are noise
326 variables). The outcome Y is then generated following one of the models and assumptions
327 described below.

328 We evaluate the performance of our method on three of its defining characteristics: 1) the
329 strong heredity property, 2) non-linearity of predictor effects and 3) interactions. Simulation
330 scenarios are designed specifically to test the performance of these characteristics.

331 1. Heredity simulation

332 Scenario (a) Truth obeys strong heredity. In this situation, the true model for Y
333 contains main effect terms for all covariates involved in interactions.

$$Y = \sum_{j=1}^4 f_j(X_j) + \beta_E \cdot X_E + X_E \cdot f_3(X_3) + X_E \cdot f_4(X_4) + \varepsilon$$

334 Scenario (b) Truth obeys weak heredity. Here, in addition to the interaction, the

4 SIMULATION STUDY

335 E variable has its own main effect but the covariates X_3 and X_4 do not.

$$Y = f_1(X_1) + f_2(X_2) + \beta_E \cdot X_E + X_E \cdot f_3(X_3) + X_E \cdot f_4(X_4) + \varepsilon$$

336 Scenario (c) Truth only has interactions. In this simulation, the covariates in-
337 volved in interactions do not have main effects as well.

$$Y = X_E \cdot f_3(X_3) + X_E \cdot f_4(X_4) + \varepsilon$$

338 2. Non-linearity simulation scenario

339 Truth is linear. **sail** is designed to model non-linearity; here we assess its per-
340 formance if the true model is completely linear.

$$Y = 5X_1 + 3(X_2 + 1) + 4X_3 + 6(X_4 - 2) + \beta_E \cdot X_E + X_E \cdot 4X_3 + X_E \cdot 6(X_4 - 2) + \varepsilon$$

341 3. Interactions simulation scenario

342 Truth only has main effects. **sail** is designed to capture interactions; here we
343 assess its performance when there are none in the true model.

$$Y = \sum_{j=1}^4 f_j(X_j) + \beta_E \cdot X_E + \varepsilon$$

344 The true component functions are the same as in [19, 21] and are given by $f_1(t) = 5t$,
345 $f_2(t) = 3(2t - 1)^2$, $f_3(t) = 4 \sin(2\pi t)/(2 - \sin(2\pi t))$, $f_4(t) = 6(0.1 \sin(2\pi t) + 0.2 \cos(2\pi t) +$
346 $0.3 \sin(2\pi t)^2 + 0.4 \cos(2\pi t)^3 + 0.5 \sin(2\pi t)^3)$. We set $\beta_E = 2$ and draw ε from a normal
347 distribution with variance chosen such that the signal-to-noise ratio is 2. Using this setup,
348 we generated 200 replications consisting of a training set of $n = 200$, a validation set of
349 $n = 200$ and a test set of $n = 800$. The training set was used to fit the model and the

4 SIMULATION STUDY

validation set was used to select the optimal tuning parameter corresponding to the minimum prediction mean squared error (MSE). Variable selection results including true positive rate, false positive rate and number of active variables (the number of variables with a non-zero coefficient estimate) were assessed on the training set, and MSE was assessed on the test set.

4.3 Results

The prediction accuracy and variable selection results for each of the five simulation scenarios are shown in Figure 3 and Table 2, respectively. We see that `sail`, `adaptive sail` and `sail weak` have the best performance in terms of both MSE and yielding correct sparse models when the truth follows a strong heredity (scenario 1a), as we would expect, since this is exactly the scenario that our method is trying to target. Our method is also competitive when only main effects are present (scenario 3) and performs just as well as methods that only consider linear and non-linear main effects (`HierBasis`, `SPAM`), owing to the penalization applied to the interaction parameter. Due to the heredity property being violated in scenario 1c), no method can identify the correct model with the exception of `GLinternet`. When only linear effects and interactions are present (scenario 2), we see that `adaptive sail` has similar MSE compared to the other linear interaction methods (`lassoBT` and `GLinternet`) with a better TPR and FPR. Overall, our simulation study results suggests that `sail` outperforms existing methods when the true model contains non-linear interactions, and is competitive even when the truth only has either linear or additive main effects.

We visually inspected whether our method could correctly capture the shape of the association between the predictors and the response for both main and interaction effects. To do so, we plotted the true and predicted curves for scenario 1a) only. Figure 4 shows each of the four main effects with the estimated curves from each of the 200 simulations along with the true curve. We can see the effect of the penalty on the parameters, i.e., decreasing prediction

4 SIMULATION STUDY

Table 2: Mean (standard deviation) of the number of selected variables ($|\hat{\mathcal{J}}|$), true positive rate (TPR) and false positive rate (FPR) as a percentage from 200 simulations for each of the five scenarios. $|\mathcal{J}|$ is the number of truly associated variables.

Linear Main Effects		Linear Interactions		Non-linear Main Effects			Non-linear Interactions			
lasso	adaptive lasso	lassoBT	GLinternet	HierBasis	SPAM	gamsel	sail	adaptive sail	sail weak	
1a) Strong heredity ($\mathcal{J} = 7$)										
$ \hat{\mathcal{J}} $	30 (14)	8 (4)	37 (17)	41 (21)	152 (28)	38 (17)	47 (19)	37 (15)	8 (5)	34 (13)
TPR	54.9 (7.4)	49.7 (10.4)	62.0 (10.4)	66.7 (12.8)	66.2 (7.6)	60.9 (9.0)	57.1 (6.5)	90.6 (7.7)	69.7 (28.8)	86.4 (10.1)
FPR	1.3 (0.7)	0.2 (0.2)	1.6 (0.8)	1.8 (1.0)	7.4 (1.4)	1.7 (0.8)	2.2 (0.9)	1.5 (0.7)	1.1 (9.7)	1.4 (0.6)
1b) Weak heredity ($\mathcal{J} = 5$)										
$ \hat{\mathcal{J}} $	19 (12)	4 (2)	20 (13)	37 (22)	23 (22)	28 (15)	22 (15)	16 (9)	7 (6)	17 (11)
TPR	41.0 (4.5)	40.2 (1.9)	41.0 (4.5)	65.1 (15.2)	42.6 (6.7)	54.8 (8.8)	43.8 (7.9)	47.8 (10.4)	46.9 (11.2)	51.0 (12.8)
FPR	0.8 (0.6)	0.1 (0.1)	0.9 (0.7)	1.7 (1.1)	1.1 (1.1)	1.3 (0.7)	1.0 (0.8)	0.7 (0.4)	0.2 (0.3)	0.7 (0.5)
1c) Interactions Only ($\mathcal{J} = 2$)										
$ \hat{\mathcal{J}} $	14 (13)	3 (2)	15 (14)	42 (21)	14 (14)	14 (12)	14 (13)	6 (7)	3 (5)	6 (7)
TPR	0.0 (0.0)	0.0 (0.0)	0.2 (3.5)	82.6 (26.3)	0.0 (0.0)	0.0 (0.0)	0.0 (0.0)	0.0 (0.0)	0.7 (5.9)	0.0 (0.0)
FPR	0.7 (0.6)	0.6 (6.9)	0.8 (0.7)	2.0 (1.1)	0.7 (0.7)	0.7 (0.6)	0.7 (0.6)	0.3 (0.4)	0.2 (0.2)	0.3 (0.4)
2) Linear Effects ($\mathcal{J} = 7$)										
$ \hat{\mathcal{J}} $	36 (16)	8 (3)	48 (17)	47 (20)	36 (17)	42 (18)	36 (16)	30 (12)	12 (4)	19 (14)
TPR	69.9 (4.7)	67.4 (6.7)	72.7 (6.6)	92.6 (9.1)	69.9 (4.6)	64.6 (8.4)	69.9 (4.7)	87.4 (14.1)	88.6 (13.5)	64.3 (13.6)
FPR	1.6 (0.8)	0.2 (0.1)	2.1 (0.8)	2.1 (1.0)	1.6 (0.9)	1.9 (0.9)	1.6 (0.8)	1.2 (0.6)	0.3 (0.2)	0.7 (0.7)
3) Main Effects Only ($\mathcal{J} = 5$)										
$ \hat{\mathcal{J}} $	30 (15)	7 (4)	31 (15)	35 (18)	160 (17)	42 (18)	54 (20)	40 (16)	8 (5)	40 (16)
TPR	76.6 (10.0)	67.4 (13.6)	77.0 (10.1)	78.3 (8.8)	97.0 (7.5)	92.3 (10.9)	82.4 (10.0)	89.3 (13.0)	78.0 (14.8)	89.1 (13.0)
FPR	1.3 (0.7)	0.2 (0.2)	1.4 (0.8)	1.6 (0.9)	7.8 (0.8)	1.9 (0.9)	2.5 (1.0)	1.8 (0.8)	0.2 (0.2)	1.8 (0.8)

375 variance at the cost of increased bias. This is particularly well illustrated in the bottom right
 376 panel where **sail** smooths out the very wiggly component function $f_4(x)$. Nevertheless, the
 377 primary shapes are clearly being captured.

378 To visualize the estimated interaction effects, we ordered the 200 simulation runs by the Eu-
 379 clidean distance between the estimated and true regression functions. Following Radchenko
 380 et al. [28], we then identified the 25th, 50th, and 75th best simulations and plotted, in Fig-
 381 ures 5 and 6, the interaction effects of X_E with $f_3(X_3)$ and $f_4(X_4)$, respectively. We see
 382 that **sail** does a good job at capturing the true interaction surface for $X_E \cdot f_3(X_3)$. Again,
 383 the smoothing and shrinkage effect is apparent when looking at the interaction surfaces for
 384 $X_E \cdot f_4(X_4)$

4 SIMULATION STUDY

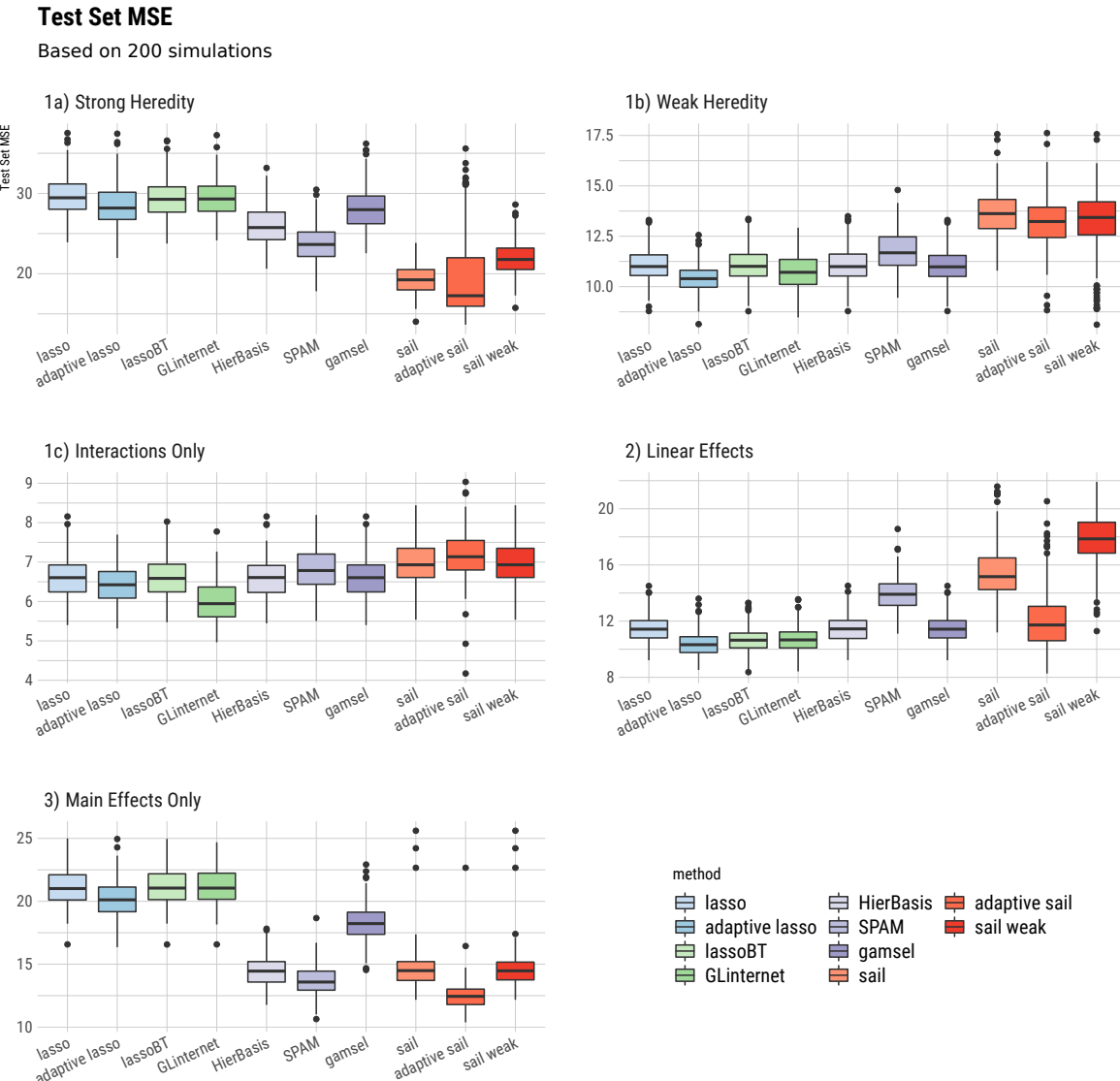


Figure 3: Boxplots of the test set mean squared error from 200 simulations for each of the five simulation scenarios.

4 SIMULATION STUDY

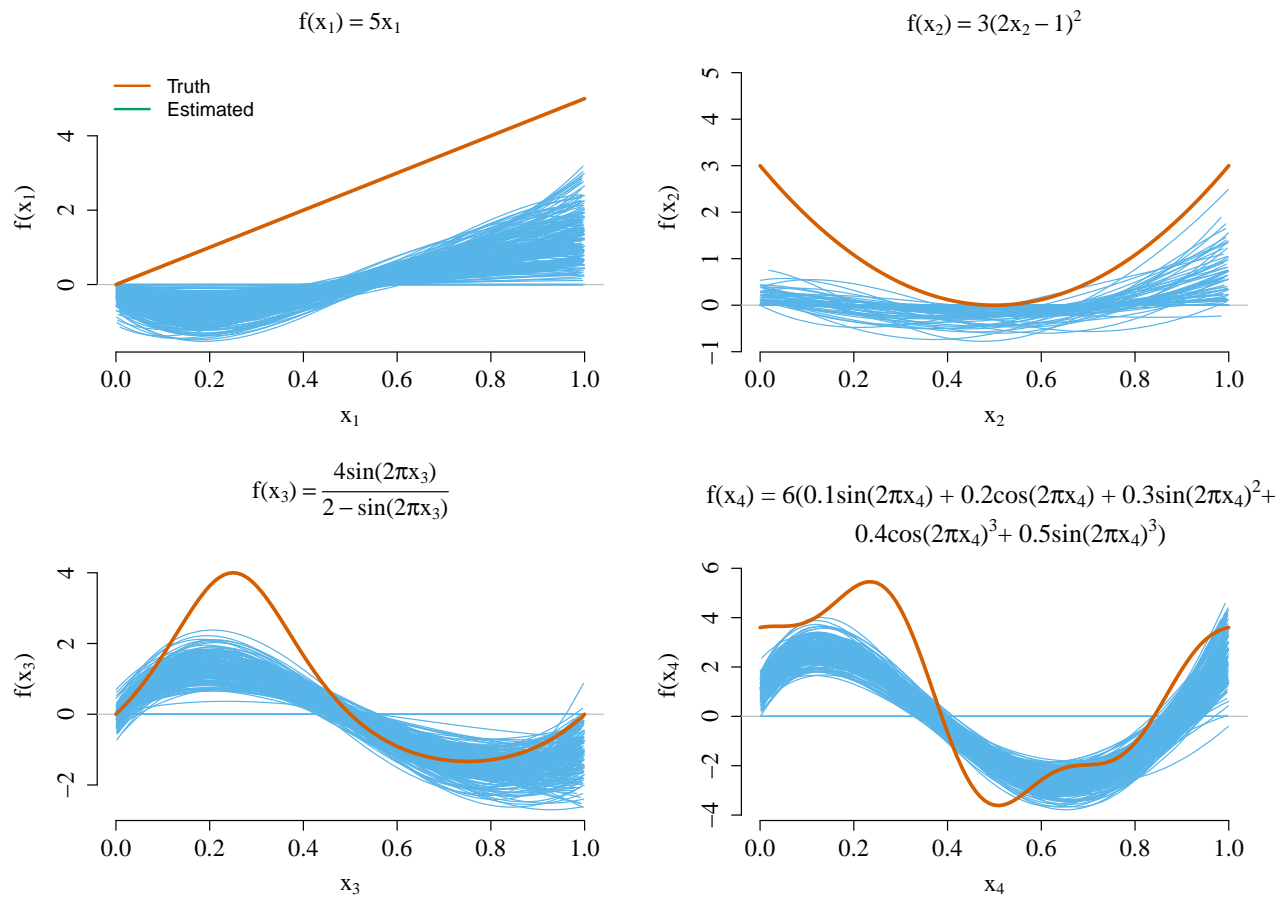


Figure 4: True and estimated main effect component functions for scenario 1a). The estimated curves represent the results from each one of the 200 simulations conducted.

4 SIMULATION STUDY

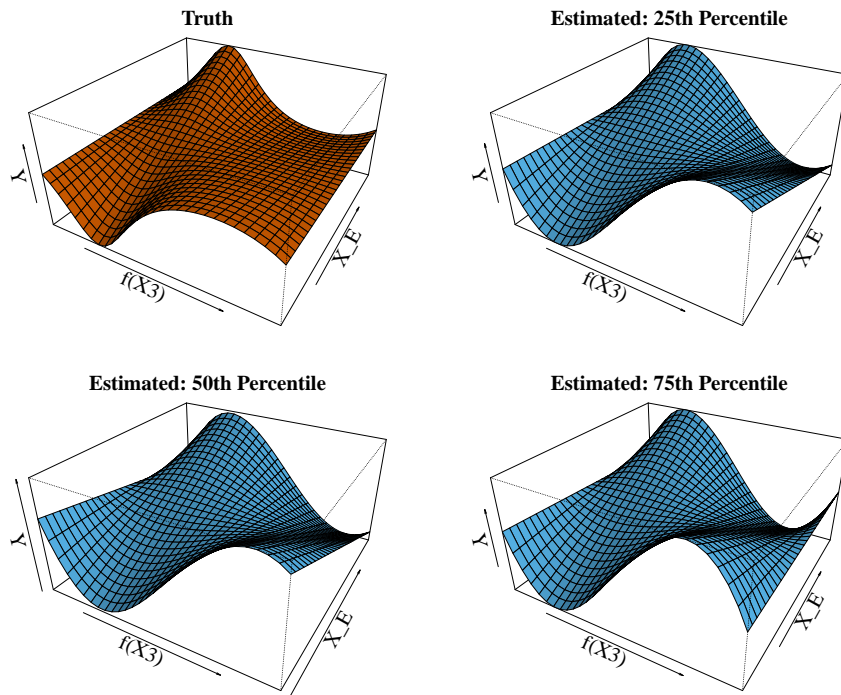


Figure 5: True and estimated interaction effects for $X_E \cdot f_3(X_3)$ in simulation scenario 1a).

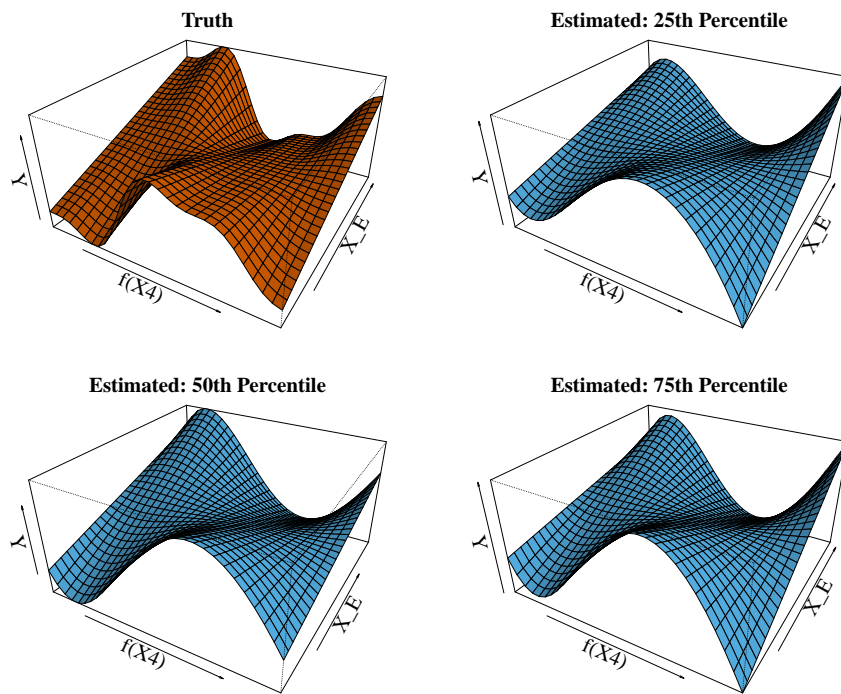


Figure 6: True and estimated interaction effects for $X_E \cdot f_4(X_4)$ in simulation scenario 1a).

5 REAL DATA APPLICATIONS

385 5 Real data applications

386 5.1 Gene-environment interactions in the Nurse Family Partnership 387 program

388 It is well known that environmental exposures can have an important impact on academic
389 achievement. Indeed, early intervention in young children has been shown to positively im-
390 pact intellectual abilities [6]. More recent studies have shown that cognitive performance,
391 a trait that measures the ability to learn, reason and solve problems, is also strongly influ-
392 enced by genetic factors. Genome-wide association studies (GWAS) suggest that 20% of the
393 variance in educational attainment (years of education) may be accounted for by common
394 genetic variation [25, 30]. Unsurprisingly, there is significant overlap in the SNPs that predict
395 educational attainment and measures of cognitive function. An interesting query that arises
396 is how the environment interacts with these genetics variants to predict measures of cognitive
397 function. To address this question, we analyzed data from the Nurse Family Partnership
398 (NFP), a psychosocial intervention program that begins in pregnancy and targets maternal
399 health, parenting and mother-infant interactions [26]. The Stanford Binet IQ scores at 4
400 years of age were collected for 189 subjects (including 19 imputed using `mice` [5]) born to
401 women randomly assigned to control ($n = 100$) or nurse-visited intervention groups ($n =$
402 89). For each subject, we calculated a polygenic risk score (PRS) for educational attainment
403 at different p-value thresholds using weights from the GWAS conducted in Okbay et al. [25].
404 In this context, individuals with a higher PRS have a propensity for higher educational at-
405 tainment. The goal of this analysis was to determine if there was an interaction between
406 genetic predisposition to educational attainment (X) and maternal participation in the NFP
407 program (E) on child IQ at 4 years of age (Y). We applied the weak heredity `sail` with
408 cubic B-splines and $\alpha = 0.1$, and selected the optimal tuning parameter using 10-fold cross-
409 validation. Our method identified an interaction between the intervention and PRS which

5 REAL DATA APPLICATIONS

410 included genetic variants at the 0.0001 level of significance. This interaction is shown in Fig-
411 ure 7. We see that the intervention has a much larger effect on IQ for lower PRS compared
412 to a higher PRS. In other words, perinatal home visitation by nurses can impact IQ scores
413 in children who are genetically predisposed to lower educational attainment. Similar results
414 were obtained for the other imputed datasets (Supplemental Section C).

415 We also compared **sail** with two other interaction selection methods, **lassoBT** and **GLinternet**
416 with default settings, on 200 bootstrap samples of the data. The average and standard de-
417 viation of the MSE and size of the active set ($|\hat{\mathcal{J}}|$) across the 200 bootstrap samples are
418 given in Table 3. We see that **sail** tends to select sparser models while maintaining similar
419 prediction performance compared to **lassoBT**. The **GLinternet** statistics are omitted here
420 since the algorithm did not converge for many of the 200 simulations.

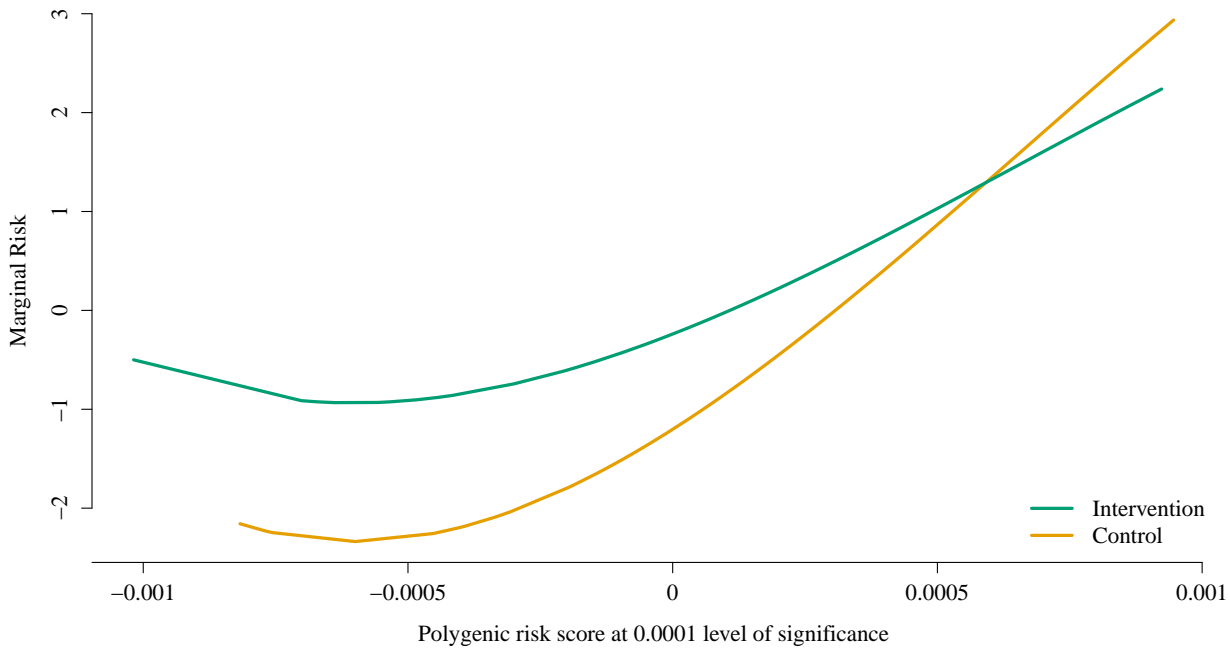


Figure 7: Estimated interaction effect identified by the weak heredity **sail** using cubic B-splines and $\alpha = 0.1$ for the Nurse Family Partnership data. The selected model, chosen via 10-fold cross-validation, contained three variables: the main effects for the intervention and the PRS for educational attainment using genetic variants significant at the 0.0001 level, as well as their interaction.

5 REAL DATA APPLICATIONS

421 5.2 Study to Understand Prognoses Preferences Outcomes and 422 Risks of Treatment

423 The Study to Understand Prognoses Preferences Outcomes and Risks of Treatment (SUP-
424 PORT) aimed at identifying which clinical variables influence medium-term (half-year) mor-
425 tality rate amongst seriously ill hospitalized patients and improving clinical decision mak-
426 ing [10]. With a relatively large sample size of 9,105 and detailed documentation of clinical
427 variables, the SUPPORT dataset allows detection of potential interactions using the strat-
428 egy implemented in **sail**. We applied **sail** to test for non-linear interactions between acute
429 renal failure or multiple organ system failure (ARF/MOSF), an important predictor for
430 survival rate, and 13 other variables that were deemed clinically relevant. These variables
431 included the number of comorbidities (excluding ARF/MOSF), age, sex, as well as multiple
432 physiological and blood biochemical indices. The response was whether a patient survived
433 after six months since hospitalization.

434 A total of 8,873 samples had complete data on all variables of interest. We randomly divided
435 these samples into equal sized training/validation/test splits and ran **lassoBT**, **GLinternet**,
436 and the weak heredity **sail** with cubic B-splines and $\alpha = 0.1$. A binomial distribution
437 family was specified for **GLinternet**, whereas **lassoBT** had the same default settings as the
438 simulation study since it did not support a specialized implementation for binary outcomes.
439 We again ran each method on the training data, determined the optimal tuning parameter
440 on the validation data based on the area under the receiver operating characteristic curve
441 (AUC), and assessed AUC on the test data. We repeated this process 200 times and report
442 the results in Table 3. We found that **sail** achieved similar prediction accuracy to **lassoBT**
443 and **GLinternet**. However, the predictive performance of **lassoBT** and **GLinternet** relied
444 on models which included many more variables. In Figure 8, we visualize the two strongest
445 interaction effects associated with the number of comorbidities and age, respectively. For
446 those having undergone ARF/MOSF, an increased number of comorbidities decreases their

6 DISCUSSION

447 chance of survival, while there seems to be no such relationship for non-ARF/MOSF patients.
448 The interaction between ARF/MOSF and age shows the risk incurred by ARF/MOSF is most
449 distinguishing among patients between the ages of 70 and 80.

Table 3: Comparison of analytic methods for selecting interactions using the Nurse Family Partnership program and the SUPPORT datasets. Averages (standard deviations in parentheses) are based on 200 bootstrap samples.

Method	Nurse Family Partnership		SUPPORT	
	Mean Squared Error	$ \widehat{\mathcal{J}} $	AUC	$ \widehat{\mathcal{H}} $
sail	3.5 (0.6)	4 (3)	0.66 (0.01)	25 (3)
lassoBT	3.53 (0.477)	11 (6)	0.65 (0.009)	49 (14)
GLinternet^a	—	—	0.65 (0.009)	58 (7)

^a **GLinternet** results not reported for NFP data since the algorithm did not converge in many of the bootstrap samples.

^b $|\widehat{\mathcal{J}}|$ is the number of variables selected by the method.

450 6 Discussion

451 In this article we have introduced the sparse additive interaction learning model **sail** for
452 detecting non-linear interactions with a key environmental or exposure variable in high-
453 dimensional settings. Using a simple reparametrization, we are able to achieve either the
454 weak or strong heredity property without using a complex penalty function. We developed
455 a blockwise coordinate descent algorithm to solve the **sail** objective function for the least-
456 squares loss. We further studied the asymptotic properties of our method and showed that
457 under certain conditions, it possesses the oracle property. All our algorithms have been
458 implemented in a computationally efficient, well-documented and freely available R package
459 on CRAN. Furthermore, our method is flexible enough to handle any type of basis expansion
460 including the identity map, which allows for linear interactions. Our implementation allows
461 the user to selectively apply the basis expansions to the predictors, allowing for example, a

6 DISCUSSION

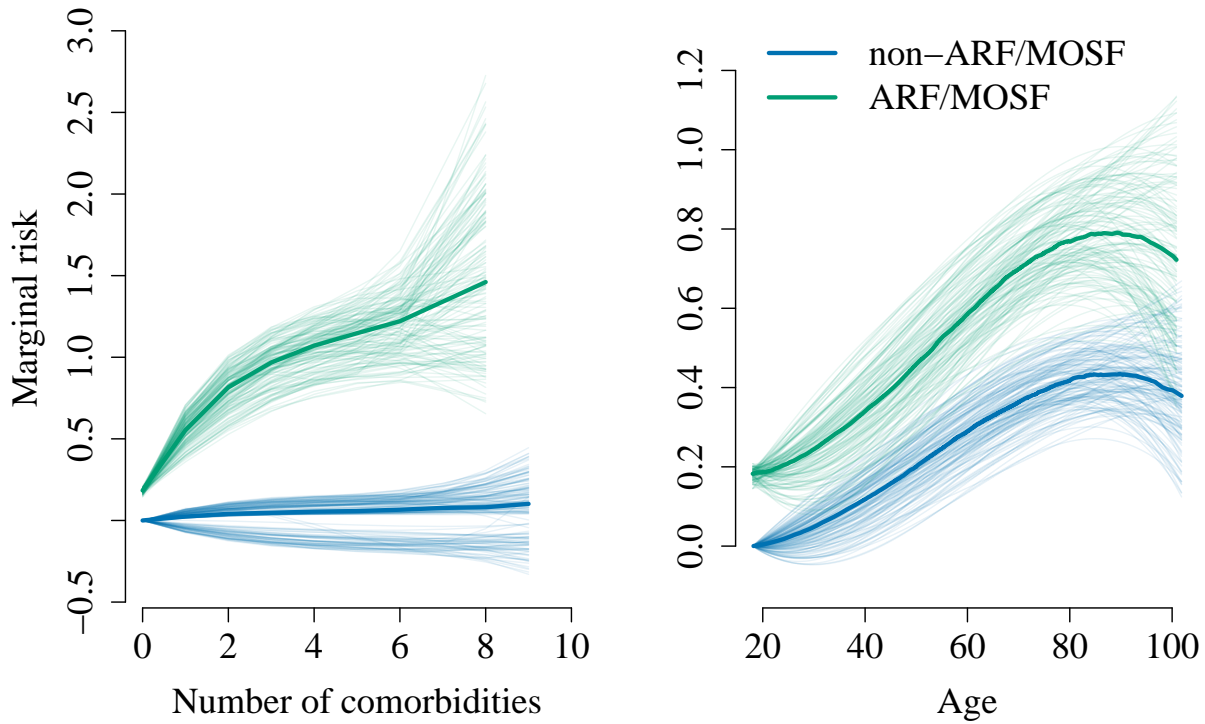


Figure 8: Illustration of estimated interaction effects identified by `sail` for the SUPPORT data. Median prediction curves in dark colors based on 200 train/validate/test splits represent the estimated marginal interaction effects. Coefficients estimated in each of the 200 train/validate/test splits were used to generate prediction curves representing a 90% confidence interval colored in corresponding light colors.

462 combination of continuous and categorical predictors. An extensive simulation study shows
463 that `sail`, `adaptive sail` and `sail weak` outperform existing penalized regression methods
464 in terms of prediction accuracy, sensitivity and specificity when there are non-linear main
465 effects only, as well as interactions with an exposure variable. We then demonstrated the
466 utility of our method to identify non-linear interactions in both biological and epidemiological
467 data. In the NFP program, we showed that individuals who are genetically predisposed to
468 lower educational attainment are those who stand to benefit the most from the intervention.
469 Analysis of the SUPPORT data revealed that those having undergone ARF/MOSF, an
470 increased number of comorbidities decreased their chances of survival, while there seemed
471 to be no such relationship for non-ARF/MOSF patients. In a bootstrap analysis of both
472 datasets, we observed that `sail`tended to select sparser models while maintaining similar

REFERENCES

473 prediction performance compared to other interaction selection methods.

474 Our method however does have its limitations. `sail` can currently only handle $X_E \cdot f(X)$ or
475 $f(X_E) \cdot X$ and does not allow for $f(X, X_E)$, i.e., only one of the variables in the interaction can
476 have a non-linear effect and we do not consider the tensor product. The reparametrization
477 leads to a non-convex optimization problem which makes convergence rates difficult to assess,
478 though we did not experience any major convergence issues in our simulations and real
479 data analysis. The memory footprint can also be an issue depending on the degree of
480 the basis expansion and the number of variables. Furthermore, the functional form of the
481 covariate effects is treated as known in our method. Being able to automatically select
482 for example, linear vs. nonlinear components, is currently an active area of research in
483 main effects models [16]. To our knowledge, our proposal is the first to allow for non-linear
484 interactions with a key exposure variable following the weak or strong heredity property
485 in high-dimensional settings. We also provide a first software implementation for these
486 models.

487

References

- 488 [1] F. Bach, R. Jenatton, J. Mairal, G. Obozinski, et al. Structured sparsity through convex
489 optimization. *Statistical Science*, 27(4):450–468, 2012. [6](#)
- 490 [2] S. R. Bhatnagar, Y. Yang, B. Khundrakpam, A. C. Evans, M. Blanchette, L. Bouchard,
491 and C. M. Greenwood. An analytic approach for interpretable predictive models in high-
492 dimensional data in the presence of interactions with exposures. *Genetic epidemiology*,
493 42(3):233–249, 2018. [3](#)
- 494 [3] J. Bien, J. Taylor, R. Tibshirani, et al. A lasso for hierarchical interactions. *The Annals*
495 *of Statistics*, 41(3):1111–1141, 2013. [6](#), [9](#)
- 496 [4] P. Bühlmann and S. Van De Geer. *Statistics for high-dimensional data: methods, theory*
497 *and applications*. Springer Science & Business Media, 2011. [5](#)

REFERENCES

- 498 [5] S. v. Buuren and K. Groothuis-Oudshoorn. mice: Multivariate imputation by chained
499 equations in r. *Journal of statistical software*, pages 1–68, 2010. 26, 21, 22
- 500 [6] F. A. Campbell and C. T. Ramey. Effects of early intervention on intellectual and
501 academic achievement: a follow-up study of children from low-income families. *Child
502 development*, 65(2):684–698, 1994. 4, 26
- 503 [7] H. Chipman. Bayesian variable selection with related predictors. *Canadian Journal of
504 Statistics*, 24(1):17–36, 1996. 5, 6
- 505 [8] N. H. Choi, W. Li, and J. Zhu. Variable selection with the strong heredity constraint and
506 its oracle property. *Journal of the American Statistical Association*, 105(489):354–364,
507 2010. 6, 9, 16, 2, 5
- 508 [9] A. Chouldechova and T. Hastie. Generalized additive model selection. *arXiv preprint
509 arXiv:1506.03850*, 2015. 18
- 510 [10] A. F. Connors, N. V. Dawson, N. A. Desbiens, W. J. Fulkerson, L. Goldman, W. A.
511 Knaus, J. Lynn, R. K. Oye, M. Bergner, A. Damiano, et al. A controlled trial to
512 improve care for seriously ill hospitalized patients: The study to understand prognoses
513 and preferences for outcomes and risks of treatments (support). *Jama*, 274(20):1591–
514 1598, 1995. 11, 28
- 515 [11] D. R. Cox. Interaction. *International Statistical Review/Revue Internationale de Statis-
516 tique*, pages 1–24, 1984. 5
- 517 [12] J. Fan, F. Han, and H. Liu. Challenges of big data analysis. *National science review*,
518 1(2):293–314, 2014. 5
- 519 [13] J. Fan and R. Li. Variable selection via nonconcave penalized likelihood and its oracle
520 properties. *Journal of the American statistical Association*, 96(456):1348–1360, 2001.
521 10, 17, 2, 5
- 522 [14] J. Friedman, T. Hastie, and R. Tibshirani. Regularization paths for generalized linear
523 models via coordinate descent. *Journal of statistical software*, 33(1):1, 2010. 11, 12, 19
- 524 [15] N. Hao, Y. Feng, and H. H. Zhang. Model selection for high-dimensional quadratic

REFERENCES

- 525 regression via regularization. *Journal of the American Statistical Association*, pages
526 1–11, 2018. 9
- 527 [16] A. Haris, A. Shojaie, and N. Simon. Nonparametric regression with adaptive truncation
528 via a convex hierarchical penalty. *arXiv preprint arXiv:1611.09972*, 2016. 18, 31
- 529 [17] A. Haris, D. Witten, and N. Simon. Convex modeling of interactions with strong
530 heredity. *Journal of Computational and Graphical Statistics*, 25(4):981–1004, 2016. 6,
531 9
- 532 [18] T. Hastie, R. Tibshirani, and M. Wainwright. *Statistical Learning with Sparsity: The*
533 *Lasso and Generalizations*. CRC Press, 2015. 4
- 534 [19] J. Huang, J. L. Horowitz, and F. Wei. Variable selection in nonparametric additive
535 models. *Annals of statistics*, 38(4):2282, 2010. 19, 20
- 536 [20] M. Lim and T. Hastie. Learning interactions via hierarchical group-lasso regularization.
537 *Journal of Computational and Graphical Statistics*, 24(3):627–654, 2015. 6, 9, 18
- 538 [21] Y. Lin, H. H. Zhang, et al. Component selection and smoothing in multivariate non-
539 parametric regression. *The Annals of Statistics*, 34(5):2272–2297, 2006. 19, 20
- 540 [22] P. McCullagh and J. A. Nelder. *Generalized linear models*, volume 37. CRC press, 1989.
541 5
- 542 [23] Y. Nardi, A. Rinaldo, et al. On the asymptotic properties of the group lasso estimator
543 for linear models. *Electronic Journal of Statistics*, 2:605–633, 2008. 17, 2
- 544 [24] K. Ning, B. Chen, F. Sun, Z. Hobel, L. Zhao, W. Matloff, A. W. Toga, A. D. N.
545 Initiative, et al. Classifying alzheimer’s disease with brain imaging and genetic data
546 using a neural network framework. *Neurobiology of aging*, 2018. 3
- 547 [25] A. Okbay, J. P. Beauchamp, M. A. Fontana, J. J. Lee, T. H. Pers, C. A. Rietveld,
548 P. Turley, G.-B. Chen, V. Emilsson, S. F. W. Meddins, et al. Genome-wide association
549 study identifies 74 loci associated with educational attainment. *Nature*, 533(7604):539,
550 2016. 26
- 551 [26] D. Olds, C. R. Henderson Jr, R. Cole, J. Eckenrode, H. Kitzman, D. Luckey, L. Pettitt,

REFERENCES

- 552 K. Sidora, P. Morris, and J. Powers. Long-term effects of nurse home visitation on
553 children's criminal and antisocial behavior: 15-year follow-up of a randomized controlled
554 trial. *Jama*, 280(14):1238–1244, 1998. [4](#), [10](#), [26](#)
- 555 [27] R Core Team. *R: A Language and Environment for Statistical Computing*. R Foundation
556 for Statistical Computing, Vienna, Austria, 2017. [19](#)
- 557 [28] P. Radchenko and G. M. James. Variable selection using adaptive nonlinear interac-
558 tion structures in high dimensions. *Journal of the American Statistical Association*,
559 105(492):1541–1553, 2010. [6](#), [9](#), [22](#)
- 560 [29] P. Ravikumar, J. Lafferty, H. Liu, and L. Wasserman. Sparse additive models. *Journal*
561 *of the Royal Statistical Society: Series B (Statistical Methodology)*, 71(5):1009–1030,
562 2009. [18](#)
- 563 [30] C. A. Rietveld, S. E. Medland, J. Derringer, J. Yang, T. Esko, N. W. Martin, H.-
564 J. Westra, K. Shakhbazov, A. Abdellaoui, A. Agrawal, et al. Gwas of 126,559 in-
565 dividuals identifies genetic variants associated with educational attainment. *science*,
566 340(6139):1467–1471, 2013. [4](#), [26](#)
- 567 [31] E. E. Schadt. Molecular networks as sensors and drivers of common human diseases.
568 *Nature*, 461(7261):218–223, 2009. [3](#)
- 569 [32] R. D. Shah. Modelling interactions in high-dimensional data with backtracking. *Journal*
570 *of Machine Learning Research*, 17(207):1–31, 2016. [9](#), [18](#)
- 571 [33] Y. She and H. Jiang. Group regularized estimation under structural hierarchy. *arXiv*
572 *preprint arXiv:1411.4691*, 2014. [9](#)
- 573 [34] R. Tibshirani. Regression shrinkage and selection via the lasso. *Journal of the Royal*
574 *Statistical Society. Series B (Methodological)*, pages 267–288, 1996. [18](#)
- 575 [35] R. Tibshirani and J. Friedman. A pliable lasso. *arXiv preprint arXiv:1712.00484*, 2017.
576 [10](#)
- 577 [36] N. J. Timpson, C. M. Greenwood, N. Soranzo, D. J. Lawson, and J. B. Richards. Genetic
578 architecture: the shape of the genetic contribution to human traits and disease. *Nature*

REFERENCES

- 579 *Reviews Genetics*, 19(2):110, 2018. [3](#)
- 580 [37] H. Wang, G. Li, and C.-L. Tsai. Regression coefficient and autoregressive order shrinkage
581 and selection via the lasso. *Journal of the Royal Statistical Society: Series B (Statistical
582 Methodology)*, 69(1):63–78, 2007. [16](#), [2](#)
- 583 [38] Y. Yang and H. Zou. A fast unified algorithm for solving group-lasso penalize learning
584 problems. *Statistics and Computing*, 25(6):1129–1141, 2015. [12](#), [19](#)
- 585 [39] P. Zhao, G. Rocha, and B. Yu. The composite absolute penalties family for grouped
586 and hierarchical variable selection. *The Annals of Statistics*, pages 3468–3497, 2009. [9](#)
- 587 [40] H. Zou. The adaptive lasso and its oracle properties. *Journal of the American statistical
588 association*, 101(476):1418–1429, 2006. [11](#), [14](#), [15](#), [17](#), [18](#)
- 589 [41] H. Zou and T. Hastie. Regularization and variable selection via the elastic net. *Journal
590 of the Royal Statistical Society: Series B (Statistical Methodology)*, 67(2):301–320, 2005.
591 [6](#)
- 592 [42] H. Zou and H. H. Zhang. On the adaptive elastic-net with a diverging number of
593 parameters. *Annals of statistics*, 37(4):1733, 2009. [17](#)

594 **A Proofs**

595 **A.1 Regularity Conditions**

596 **(C1)** The observation $\{\mathbf{V}_i : i = 1, \dots, n\}$ are independent and identically distributed with
 597 a probability density $f(\mathbf{V}, \Phi)$, which has a common support. We assume the density
 598 f satisfies the following equations:

$$E_{\Phi} \left[\nabla_{\phi_j} \log f(\mathbf{V}, \Phi) \right] = \mathbf{0} \quad \text{for } j = 1, \dots, 2p + 1.$$

and

$$\begin{aligned} \mathbf{I}_{j_1 k_1 j_2 k_2}(\Phi) &= E_{\Phi} \left[\frac{\partial}{\partial \phi_{j_1 k_1}} \log f(V, \Phi) \cdot \frac{\partial}{\partial \phi_{j_2 k_2}} \log f(V, \Phi) \right] \\ &= E_{\Phi} \left[-\frac{\partial^2}{\partial \phi_{j_1 k_1} \partial \phi_{j_2 k_2}} \log f(V, \Phi) \right], \end{aligned}$$

599 for any $j_1, j_2 = 1, \dots, 2p + 1$, and $k_1 = 1, \dots, p_{j_1}$, $k_2 = 1, \dots, p_{j_2}$, where j_1, j_2 are the
 600 index of group, k_1, k_2 be the index of elements within the corresponding group, p_{j_1}, p_{j_2}
 601 are the group size of j_1, j_2 respectively.

602 **(C2)** The Fisher information matrix

$$\mathbf{I}(\Phi) = E \left[\left(\frac{\partial}{\partial \Phi} \log f(V, \Phi) \right) \left(\frac{\partial}{\partial \Phi} \log f(V, \Phi) \right)^{\top} \right]$$

603 is finite and positive definite at $\Phi = \Phi^*$.

604 **(C3)** There exists an open set ω of Ω that contains the true parameter point Φ^* such that
 605 for almost all \mathbf{V} the density $f(\mathbf{V}, \Phi)$ admits all third derivatives $\frac{\partial^3 f(\mathbf{V}, \Phi)}{\partial \phi_{j_1 k_1} \partial \phi_{j_2 k_2} \partial \phi_{j_3 k_3}}$ for
 606 all Φ in ω and any $j_1, j_2, j_3 = 1, \dots, 2p + 1$, and $k_1 = 1, \dots, p_{j_1}$, $k_2 = 1, \dots, p_{j_2}$ and

A PROOFS

607 $k_3 = 1, \dots, p_{j3}$. Furthermore, there exist functions $M_{j_1 k_1 j_2 k_2 j_3 k_3}$ such that

$$\left| \frac{\partial^3}{\partial \phi_{j_1 k_1} \partial \phi_{j_2 k_2} \partial \phi_{j_3 k_3}} \log f(\mathbf{V}, \boldsymbol{\Phi}) \right| \leq M_{j_1 k_1 j_2 k_2 j_3 k_3}(\mathbf{V}) \quad \text{for all } \boldsymbol{\Phi} \in \omega,$$

608 and $m_{j_1 k_1 j_2 k_2 j_3 k_3} = E_{\boldsymbol{\Phi}^*}[M_{j_1 k_1 j_2 k_2 j_3 k_3}(\mathbf{V})] < \infty$.

609 A.2 Lemma (1) proof

610 Let $\eta_n = \frac{1}{\sqrt{n}} + a_n$ and $\{\boldsymbol{\Phi}^* + \eta_n \boldsymbol{\delta} : \|\boldsymbol{\delta}\|_2 \leq C\}$ be the ball around $\boldsymbol{\Phi}^*$ for $\boldsymbol{\delta} \in \mathbb{R}^d$, where d is the
 611 dimension of the design matrix and C is some constant. Under the regularity assumptions,
 612 we show that there exists a local minimizer $\widehat{\boldsymbol{\Phi}}_n$ of $Q_n(\boldsymbol{\Phi})$ such that $\|\widehat{\boldsymbol{\Phi}}_n - \boldsymbol{\Phi}^*\|_2 = O_p(\frac{1}{\sqrt{n}})$.
 613 For this proof, we adopt the approaches outlined in [8, 13, 23, 37] and extend it to our
 614 situation. Let $\eta_n = \frac{1}{\sqrt{n}} + a_n$ and $\{\boldsymbol{\Phi}^* + \eta_n \boldsymbol{\delta} : \|\boldsymbol{\delta}\|_2 \leq C\}$ be the ball around $\boldsymbol{\Phi}^*$ for
 615 $\boldsymbol{\delta} = (\mathbf{u}_1^\top, \mathbf{u}_2^\top, \dots, \mathbf{u}_{p+1}^\top, \mathbf{u}_{p+2}^\top, \dots, \mathbf{u}_{2p+1}^\top)^\top \in \mathbb{R}^d$, where d is the dimension of the design
 616 matrix and C is some constant. The objective function is given by

$$Q_n(\boldsymbol{\Phi}) = -L_n(\boldsymbol{\Phi}) + n\lambda_m \sum_{m=1}^{2p+1} \|\boldsymbol{\phi}_m\|_2,$$

617 Define

$$D_n(\boldsymbol{\delta}) \equiv Q_n(\boldsymbol{\Phi}^* + \eta_n \boldsymbol{\delta}) - Q_n(\boldsymbol{\Phi}^*).$$

A PROOFS

Then for $\boldsymbol{\delta}$ that satisfies $\|\boldsymbol{\delta}\|_2 = C$, we have

$$\begin{aligned}
 D_n(\boldsymbol{\delta}) &= -L_n(\Phi^* + \eta_n \boldsymbol{\delta}) + L_n(\Phi^*) + n \sum_{m=1}^{2p+1} \lambda_m (\|\boldsymbol{\theta}_m^* + \eta_n \mathbf{u}_m\|_2 - \|\boldsymbol{\theta}_m^*\|_2) \\
 &\stackrel{(a)}{\geq} -L_n(\Phi^* + \eta_n \boldsymbol{\delta}) + L_n(\Phi^*) + n \sum_{m \in \mathcal{A}_1} \lambda_m^\theta (\|\boldsymbol{\theta}_m^* + \eta_n \mathbf{u}_m\|_2 - \|\boldsymbol{\theta}_m^*\|_2) \\
 &\quad + n \sum_{m \in \mathcal{A}_2} \lambda_m^\theta (\|\boldsymbol{\theta}_m^* + \eta_n \mathbf{u}_m\|_2 - \|\boldsymbol{\theta}_m^*\|_2) \\
 &\stackrel{(b)}{\geq} -L_n(\Phi^* + \eta_n \boldsymbol{\delta}) + L_n(\Phi^*) - n\eta_n \sum_{m \in \mathcal{A}_1} \lambda_m \|\mathbf{u}_m\|_2 - n\eta_n \sum_{m \in \mathcal{A}_2} \lambda_m \|\mathbf{u}_m\|_2 \\
 &\stackrel{(c)}{\geq} -L_n(\Phi^* + \eta_n \boldsymbol{\delta}) + L_n(\Phi^*) - n\eta_n^2 \sum_{m \in \mathcal{A}_1} \|\mathbf{u}_m\|_2 - n\eta_n^2 \sum_{m \in \mathcal{A}_2} \|\mathbf{u}_m\|_2 \\
 &\geq -L_n(\Phi^* + \eta_n \boldsymbol{\delta}) + L_n(\Phi^*) - n\eta_n^2 (|\mathcal{A}_1| + |\mathcal{A}_2|)C \\
 &\stackrel{(d)}{=} -[\nabla L_n(\Phi^*)]^\top (\eta_n \boldsymbol{\delta}) - \frac{1}{2} (\eta_n \boldsymbol{\delta})^\top [\nabla^2 L_n(\Phi^*)] (\eta_n \boldsymbol{\delta}) (1 + o(1)) \\
 &\quad - n\eta_n^2 (|\mathcal{A}_1| + |\mathcal{A}_2|)C
 \end{aligned} \tag{15}$$

Inequality (a) is by the fact that $\sum_{m \notin \mathcal{A}_1} \|\boldsymbol{\phi}_m^*\|_2 = 0$ and $\sum_{m \notin \mathcal{A}_2} \|\boldsymbol{\phi}_m^*\|_2 = 0$. Inequality (b) is due to the reverse triangle inequality $\|a\|_2 - \|b\|_2 \geq -\|a - b\|_2$. Inequality (c) is by $\lambda_m \leq a_n \leq \eta_n$ for $m \in \mathcal{A}_1$ and $m \in \mathcal{A}_2$. Equality (d) is by the standard argument on the Taylor expansion of the loss function:

$$\begin{aligned}
 L_n(\Phi^* + \eta_n \boldsymbol{\delta}) &= L_n(\Phi^* + \eta_n \cdot \mathbf{0}) + \eta_n \nabla L_n(\Phi^* + \eta_n \cdot \mathbf{0})^\top (\boldsymbol{\delta} - \mathbf{0}) \\
 &\quad + \frac{1}{2} (\boldsymbol{\delta} - \mathbf{0})^\top \nabla^2 L_n(\Phi^* + \eta_n \cdot \mathbf{0}) (\boldsymbol{\delta} - \mathbf{0}) \{1 + o(1)\} \\
 &= L_n(\Phi^*) + \eta_n \nabla L_n(\Phi^*)^\top \boldsymbol{\delta} + \frac{1}{2} \boldsymbol{\delta}^\top \nabla^2 L_n(\Phi^*) \boldsymbol{\delta} \eta_n^2 \{1 + o(1)\}
 \end{aligned}$$

A PROOFS

⁶¹⁸ We split (15) into three parts:

$$\begin{aligned} D_1 &= -[\nabla L_n(\Phi^*)]^\top (\eta_n \boldsymbol{\delta}) \\ D_2 &= -\frac{1}{2} (\eta_n \boldsymbol{\delta})^\top [\nabla^2 L_n(\Phi^*)] (\eta_n \boldsymbol{\delta}) (1 + o(1)) \\ D_3 &= -n\eta_n^2 (|\mathcal{A}_1| + |\mathcal{A}_2|) C \end{aligned}$$

Then

$$\begin{aligned} D_1 &= -\eta_n [\nabla L_n(\Phi^*)]^\top \boldsymbol{\delta} \\ &= -\sqrt{n}\eta_n \left(\frac{1}{\sqrt{n}} \nabla L_n(\Phi^*) \right)^\top \boldsymbol{\delta} \\ &= -\sqrt{n}\eta_n \left(\sqrt{n} \frac{1}{n} \sum_{i=1}^n \nabla \log f(\mathbf{V}_i, \Phi) |_{\Phi=\Phi^*} \right)^\top \boldsymbol{\delta} \\ &= -\sqrt{n}\eta_n \left(\sqrt{n} \left[\frac{1}{n} \sum_{i=1}^n \nabla \log f(\mathbf{V}_i, \Phi) |_{\Phi=\Phi^*} - \mathbf{0} \right] \right)^\top \boldsymbol{\delta} \\ &= -\sqrt{n}\eta_n \left(\sqrt{n} \left[\frac{1}{n} \sum_{i=1}^n \nabla \log f(\mathbf{V}_i, \Phi) |_{\Phi=\Phi^*} - E_{\Phi^*} \nabla L(\Phi^*) \right] \right)^\top \boldsymbol{\delta} \\ &= -\sqrt{n}\eta_n O_P(1) \boldsymbol{\delta} \\ &= -O_P(n\eta_n^2) \boldsymbol{\delta} \end{aligned} \tag{16}$$

The last equation is by $a_n = o(\frac{1}{\sqrt{n}})$ and

$$\begin{aligned} O_P(n\eta_n^2) &= O_P(n(n^{-1/2} + a_n)^2) = O_P(1 + 2n^{1/2}a_n + na_n^2)) \\ &= O_P(1 + n^{1/2}a_n + (n^{1/2}a_n)^2) = O_P(1 + n^{1/2}a_n + o(1)) \\ &= O_p(n^{1/2}(n^{-1/2} + a_n)) = O_p(n^{1/2}\eta_n) \end{aligned}$$

A PROOFS

$$\begin{aligned}
 D_2 &= \frac{1}{2}n\eta_n^2 \left\{ \boldsymbol{\delta}^\top \left[-\frac{1}{n}\nabla^2 L_n(\Phi^*) \right] \boldsymbol{\delta} \right\} (1 + o_p(1)) \\
 &= \frac{1}{2}n\eta_n^2 \{ \boldsymbol{\delta}^\top [\mathbf{I}(\Phi^*)] \boldsymbol{\delta} \} (1 + o_p(1)) \text{ by the weak law of large numbers.} \\
 &= O_p(n\eta_n^2 \|\boldsymbol{\delta}\|_2^2)
 \end{aligned} \tag{17}$$

619 Combining (16) and (17) with (15) gives:

$$\begin{aligned}
 D_n(\boldsymbol{\delta}) &\geq D_1 + D_2 + D_3 \\
 &= -O_P(n\eta_n^2) \boldsymbol{\delta} + O_p(n\eta_n^2 \|\boldsymbol{\delta}\|_2^2) - n\eta_n^2(|\mathcal{A}_1| + |\mathcal{A}_2|)C
 \end{aligned}$$

620 We can see that the first term D_1 is linear in $\boldsymbol{\delta}$ and the second term D_2 is quadratic in $\boldsymbol{\delta}$.

621 We can conclude that for a large enough constant $C = \|\boldsymbol{\delta}\|_2$, D_2 dominates D_1 and D_3 . Note
622 that this is a positive term since $I(\Phi)$ is positive definite at $\Phi = \Phi^*$ by regularity condition
623 (C2). Therefore, for each $\varepsilon > 0$, there exists a large enough constant C such that, for large
624 enough n

$$P \left\{ \inf_{\|\boldsymbol{\delta}\|_2=C} D_n(\boldsymbol{\delta}) > 0 \right\} \geq 1 - \varepsilon$$

625 This implies with probability at least $1 - \varepsilon$ that the empirical likelihood Q_n has a local
626 minimizer in the ball $\{\Phi^* + \eta_n \boldsymbol{\delta} : \|\boldsymbol{\delta}\|_2 \leq C\}$ (since Q_n is bounded and $\{\Phi^* + \alpha_n \boldsymbol{\delta} : \|\boldsymbol{\delta}\|_2 \leq C\}$
627 is closed). In other words, there exists a local solution $\widehat{\Phi}_n$ such that $\|\widehat{\Phi}_n - \Phi^*\| \leq \eta_n \|\boldsymbol{\delta}\|_2 \leq$
628 $\eta_n C = O_P(\eta_n) = O_P(\frac{1}{\sqrt{n}} + a_n) = O_p(\frac{1}{\sqrt{n}})$, since $a_n = o(\frac{1}{\sqrt{n}})$. Hence, $\|\widehat{\Phi}_n - \Phi^*\|_2 = O_P\left(\frac{1}{\sqrt{n}}\right)$.

629 \square

630 A.3 Theorem 1 proof

631 We first consider consistency for the main effects $P(\widehat{\Phi}_{\mathcal{A}_1^c} = \mathbf{0}) \rightarrow 1$. Following [8, 13], it is
632 sufficient to show that for all $m \in \mathcal{A}_1^c$, $P(\widehat{\phi}_m = \mathbf{0}) \rightarrow 1$, which implies that $P(\widehat{\Phi}_{\mathcal{A}_1^c} = \mathbf{0}) \rightarrow$

A PROOFS

⁶³³ 1, i.e., the \sqrt{n} -consistent estimate $\widehat{\Phi}$ has oracle property $\widehat{\phi}_m = \mathbf{0}$ if $\phi_m^* = \mathbf{0}$. Denote

$$\widehat{\phi}_m = (\widehat{\phi}_{m1}, \dots, \widehat{\phi}_{mp_m}),$$

where p_m is the group size of $\widehat{\phi}_m$. Let $\widehat{\phi}_{mk}$ be the k -th entry of $\widehat{\phi}_m$. Note that if $\widehat{\phi}_m \neq \mathbf{0}$, then $\widehat{\phi}_{mk} \neq 0$ for $k = 1, \dots, p_m$, then penalty function $\|\widehat{\phi}_m\|_2$ becomes differentiable. Therefore ϕ_{mk} for $k = 1, \dots, p_m$ must satisfy the following normal equation

$$\begin{aligned} \frac{\partial Q_n(\widehat{\Phi}_n)}{\partial \phi_{mk}} &= -\frac{\partial L_n(\widehat{\Phi}_n)}{\partial \phi_{mk}} + n\lambda_m \frac{\widehat{\phi}_{mk}}{\|\widehat{\phi}_m\|_2} \\ &= -\frac{\partial L_n(\Phi^*)}{\partial \phi_{mk}} - \sum_{j_1=1}^{2p+1} \sum_{k_1=1}^{p_{j_1}} \frac{\partial^2 L_n(\Phi^*)}{\partial \phi_{mk} \partial \phi_{j_1 k_1}} (\widehat{\phi}_{j_1 k_1} - \phi_{j_1 k_1}^*) \\ &\quad - \frac{1}{2} \sum_{j_1=1}^{2p+1} \sum_{k_1=1}^{p_{j_1}} \sum_{j_2=1}^{2p+1} \sum_{k_2=1}^{p_{j_2}} \frac{\partial^3 L_n(\widetilde{\Phi})}{\partial \phi_{mk} \partial \phi_{j_1 k_1} \partial \phi_{j_2 k_2}} (\widehat{\phi}_{j_1 k_1} - \phi_{j_1 k_1}^*) (\widehat{\phi}_{j_2 k_2} - \phi_{j_2 k_2}^*) \\ &\quad + n\lambda_m \frac{\widehat{\phi}_{mk}}{\|\widehat{\phi}_m\|_2} \triangleq I_1 + I_2 + I_3 + I_4 = 0 \end{aligned}$$

⁶³⁴ where $\widetilde{\Phi}$ lies between $\widehat{\Phi}_n$ and Φ^* . By the regularity conditions and Lemma (1) that
⁶³⁵ $\|\widehat{\Phi}_n - \Phi^*\|_2 = O_P\left(\frac{1}{\sqrt{n}}\right)$, the first term is of the order $O_p(\sqrt{n})$

$$I_1 = -\frac{\partial L_n(\widehat{\Phi}_n)}{\partial \phi_{mk}} = -\sqrt{n}\sqrt{n}\frac{1}{n} \frac{\partial L_n(\widehat{\Phi}_n)}{\partial \phi_{mk}} = \sqrt{n}O_p(1) = O_p(\sqrt{n}).$$

Then the second is of the order $O_P\left(\frac{1}{\sqrt{n}}\right)$ and the third term is of the order $O_P\left(\frac{1}{n}\right)$.

Hence

$$\frac{\partial Q_n(\widehat{\Phi}_n)}{\partial \Phi_m} = \sqrt{n} \left\{ O_p(1) + \sqrt{n}\lambda_m \frac{\widehat{\phi}_{mk}}{\|\widehat{\phi}_m\|_2} \right\}. \quad (18)$$

⁶³⁶ As $\sqrt{n}\lambda_m \geq \sqrt{n}b_n \rightarrow \infty$ for $m \in \mathcal{A}_1^c$ from the assumption, therefore we know that I_4
⁶³⁷ dominates I_1, I_2 and I_3 in (18) with probability tending to one. This means that (18) cannot

A PROOFS

be true as long as the sample size is sufficiently large. As a result, we can conclude that with probability tending to one, the estimate $\hat{\boldsymbol{\phi}}_m = (\hat{\phi}_{m1}, \dots, \hat{\phi}_{mp_m})$ must be in a position where $\hat{\boldsymbol{\phi}}_m$ is not differentiable. Hence $\hat{\boldsymbol{\phi}}_m = \mathbf{0}$ for all $m \in \mathcal{A}_1^c$. Hence $P(\hat{\Phi}_{\mathcal{A}_1^c} = \mathbf{0}) \rightarrow 1$.

This completes the proof.

Next, we prove that for the interactions $P(\hat{\Phi}_{\mathcal{A}_2^c} = \mathbf{0}) \rightarrow 1$. For $m \in \mathcal{A}_2^c$ s.t. $\boldsymbol{\phi}_m^* = \gamma_{jE}^* = 0$ but $\beta_E \neq 0$ and $\boldsymbol{\theta}_j^* \neq \mathbf{0}$ ($1 \leq j \leq p$), we can prove $P(\hat{\Phi}_{\mathcal{A}_2^c} = \mathbf{0}) \rightarrow 1$ by a similar reasoning, which further implies that $P(\hat{\gamma}_{jE} = 0) \rightarrow 0$. For $m \in \mathcal{A}_2^c$ such that $\boldsymbol{\phi}_m^* = \gamma_{jE}^* = 0$ and either $\beta_E = 0$ or $\boldsymbol{\theta}_j^* = \mathbf{0}$ ($1 \leq j \leq p$): without loss of generality, assume that $\boldsymbol{\theta}_j^* = \mathbf{0}$. Notice that $\hat{\boldsymbol{\theta}}_j = \mathbf{0}$ implies $\hat{\gamma}_{jE} = 0$, since if $\hat{\gamma}_{jE} \neq 0$, the value of the loss function does not change but the value of the penalty function will increase. Because we already prove $P(\hat{\Phi}_{\mathcal{A}_1^c} = \mathbf{0}) \rightarrow 1$, therefore we get $P(\hat{\Phi}_{\mathcal{A}_2^c} = \mathbf{0}) \rightarrow 1$ as well for this case.

□

650 A.4 Theorem 2 proof

By Lemma (1) and Theorem (1), there exists a $\hat{\Phi}_{\mathcal{A}}$ that is a \sqrt{n} -consistent local minimizer of $Q(\Phi_{\mathcal{A}})$, therefore $\left\| \hat{\Phi}_{\mathcal{A}} - \Phi_{\mathcal{A}}^* \right\|_2 = O_P\left(\frac{1}{\sqrt{n}}\right)$ and $P(\hat{\Phi}_{\mathcal{A}^c} = \mathbf{0}) \rightarrow 1$. Thus satisfies (with probability tending to 1):

$$\left. \frac{\partial Q_n(\Phi_{\mathcal{A}})}{\partial \Phi_m} \right|_{\Phi=\begin{pmatrix} \hat{\Phi}_{\mathcal{A}} \\ 0 \end{pmatrix}} = 0, \quad \forall m \in \mathcal{A}, \quad (19)$$

that is

$$\left. \frac{\partial Q_n(\Phi_{\mathcal{A}})}{\partial \Phi_m} \right|_{\Phi_{\mathcal{A}}=\hat{\Phi}_{\mathcal{A}}} = 0, \quad \forall m \in \mathcal{A}, \quad (20)$$

A PROOFS

where

$$\begin{aligned}
 Q_n(\Phi_{\mathcal{A}}) &= -L_n(\Phi_{\mathcal{A}}) + n \underbrace{\sum_{m \in \mathcal{A}_1} \lambda_m \|\phi_m\|_2 + n \sum_{m \in \mathcal{A}_2} \lambda_m \|\phi_m\|_2}_{\triangleq nP(\Phi_{\mathcal{A}})} \\
 &= -L_n(\Phi_{\mathcal{A}}) + nP(\Phi_{\mathcal{A}}). \tag{21}
 \end{aligned}$$

655 From (20) and (21) we have

$$\nabla_{\mathcal{A}} Q_n(\widehat{\Phi}_{\mathcal{A}}) = -\nabla_{\mathcal{A}} L_n(\widehat{\Phi}_{\mathcal{A}}) + n \nabla_{\mathcal{A}} P(\widehat{\Phi}_{\mathcal{A}}) = \mathbf{0}, \tag{22}$$

656 with probability tending to 1.

657 Denote $\Sigma = \text{diag}\{o_p(1), \dots, o_p(1)\}$. We then expand $-\nabla_{\mathcal{A}} L_n(\Phi_{\mathcal{A}})$ at $\Phi_{\mathcal{A}} = \Phi_{\mathcal{A}}^*$ in (22):

$$\begin{aligned}
 -\nabla_{\mathcal{A}} L_n(\widehat{\Phi}_{\mathcal{A}}) &= -\nabla_{\mathcal{A}} L_n(\Phi_{\mathcal{A}}^*) - [\nabla_{\mathcal{A}}^2 L_n(\Phi_{\mathcal{A}}^*) + \Sigma] (\widehat{\Phi}_{\mathcal{A}} - \Phi_{\mathcal{A}}^*) \\
 &= \sqrt{n} \left[-\frac{1}{\sqrt{n}} \nabla_{\mathcal{A}} L_n(\Phi_{\mathcal{A}}^*) + \left(-\frac{1}{n} \nabla_{\mathcal{A}}^2 L_n(\Phi_{\mathcal{A}}^*) - \Sigma \right) \sqrt{n} (\widehat{\Phi}_{\mathcal{A}} - \Phi_{\mathcal{A}}^*) \right] \\
 &= \sqrt{n} \left[-\frac{1}{\sqrt{n}} \nabla_{\mathcal{A}} L_n(\Phi_{\mathcal{A}}^*) + (\mathbf{I}(\Phi_{\mathcal{A}}^*) - \Sigma) \sqrt{n} (\widehat{\Phi}_{\mathcal{A}} - \Phi_{\mathcal{A}}^*) \right].
 \end{aligned}$$

658 The third line follows by

$$\frac{1}{n} \nabla_{\mathcal{A}}^2 L_n(\Phi_{\mathcal{A}}^*) = E \{ \nabla_{\mathcal{A}}^2 L(\Phi_{\mathcal{A}}^*) \} + \Sigma = -\mathbf{I}(\Phi_{\mathcal{A}}^*) + \Sigma.$$

659 Denote

$$\mathbf{b} = (\lambda_m \text{sgn}(\beta_m^*), \lambda_m \frac{\boldsymbol{\theta}_m^*}{\|\boldsymbol{\theta}_m^*\|_2}^\top, \lambda_m \text{sgn}(\gamma_{mE}^*))^\top, \quad m \in \mathcal{A},$$

We also expand $n \nabla_{\mathcal{A}} P(\Phi_{\mathcal{A}})$ at $\Phi_{\mathcal{A}} = \Phi_{\mathcal{A}}^*$ in (22):

$$n \nabla_{\mathcal{A}} P(\widehat{\Phi}_{\mathcal{A}}) = n \left[\mathbf{b} + \Sigma (\widehat{\Phi}_{\mathcal{A}} - \Phi_{\mathcal{A}}^*) \right].$$

B ALGORITHM DETAILS

And due to the fact that $\sqrt{n}\lambda_m \leq \sqrt{n}a_n \rightarrow 0$ for $m \in \mathcal{A}$ and $\frac{\theta_{mk}^*}{\|\theta_m^*\|_2} \leq 1$ for any $1 \leq k \leq p_m$, we know that $\sqrt{n}\mathbf{b} = (o_p(1), \dots, o_p(1))^\top$. Thus,

$$\begin{aligned}\nabla_{\mathcal{A}} Q_n(\widehat{\Phi}_{\mathcal{A}}) &= \sqrt{n} \left[-\frac{1}{\sqrt{n}} \nabla_{\mathcal{A}} L_n(\Phi_{\mathcal{A}}^*) + (\mathbf{I}(\Phi_{\mathcal{A}}^*) + \Sigma) \sqrt{n} (\widehat{\Phi}_{\mathcal{A}} - \Phi_{\mathcal{A}}^*) \right] \\ &\quad + \sqrt{n} [\sqrt{n}\mathbf{b} + \Sigma \sqrt{n} (\widehat{\Phi}_{\mathcal{A}} - \Phi_{\mathcal{A}}^*)] \\ &= \sqrt{n} \left[-\frac{1}{\sqrt{n}} \nabla_{\mathcal{A}} L_n(\Phi_{\mathcal{A}}^*) + \sqrt{n}\mathbf{b} + (\mathbf{I}(\Phi_{\mathcal{A}}^*) + \Sigma) \sqrt{n} (\widehat{\Phi}_{\mathcal{A}} - \Phi_{\mathcal{A}}^*) \right] \\ &= \mathbf{0}.\end{aligned}$$

660

$$(\mathbf{I}(\Phi_{\mathcal{A}}^*) + \Sigma) \sqrt{n} (\widehat{\Phi}_{\mathcal{A}} - \Phi_{\mathcal{A}}^*) = \sqrt{n} \frac{1}{n} \sum_{i=1}^n \nabla_{\mathcal{A}} \log f(\mathbf{V}_i, \Phi_{\mathcal{A}}^*) + o_p(1).$$

661 Therefore, by the central limit theorem, we know that

$$\sqrt{n} \left[\frac{1}{n} \sum_{i=1}^n \nabla_{\mathcal{A}} \log f(\mathbf{V}_i, \Phi_{\mathcal{A}}^*) \right] \rightarrow N(\mathbf{0}, \mathbf{I}(\Phi_{\mathcal{A}}^*)).$$

662 Hence,

$$\sqrt{n} (\widehat{\Phi}_{\mathcal{A}} - \Phi_{\mathcal{A}}^*) \xrightarrow{d} N(\mathbf{0}, \mathbf{I}^{-1}(\Phi_{\mathcal{A}}^*)).$$

663 \square

664 B Algorithm Details

665 In this section we provide more specific details about the algorithms used to solve the **sail** ob-
666 jective function. The strong heredity **sail** model with least-squares loss has the form

$$\hat{Y} = \beta_0 \cdot \mathbf{1} + \sum_{j=1}^p \Psi_j \boldsymbol{\theta}_j + \beta_E X_E + \sum_{j=1}^p \gamma_j \beta_E(X_E \circ \Psi_j) \boldsymbol{\theta}_j \quad (23)$$

B ALGORITHM DETAILS

⁶⁶⁷ and the objective function is given by

$$Q(\boldsymbol{\Phi}) = \frac{1}{2n} \left\| Y - \hat{Y} \right\|_2^2 + \lambda(1 - \alpha) \left(w_E |\beta_E| + \sum_{j=1}^p w_j \|\boldsymbol{\theta}_j\|_2 \right) + \lambda\alpha \sum_{j=1}^p w_{jE} |\gamma_j| \quad (24)$$

Solving (24) in a blockwise manner allows us to leverage computationally fast algorithms for ℓ_1 and ℓ_2 norm penalized regression. Denote the n -dimensional residual column vector $R = Y - \hat{Y}$. The subgradient equations are given by

$$\frac{\partial Q}{\partial \beta_0} = \frac{1}{n} \left(Y - \beta_0 \cdot \mathbf{1} - \sum_{j=1}^p \boldsymbol{\Psi}_j \boldsymbol{\theta}_j - \beta_E X_E - \sum_{j=1}^p \gamma_j \beta_E (X_E \circ \boldsymbol{\Psi}_j) \boldsymbol{\theta}_j \right)^\top \mathbf{1} = 0 \quad (25)$$

$$\frac{\partial Q}{\partial \beta_E} = -\frac{1}{n} \left(X_E + \sum_{j=1}^p \gamma_j (X_E \circ \boldsymbol{\Psi}_j) \boldsymbol{\theta}_j \right)^\top R + \lambda(1 - \alpha) w_E s_1 = 0 \quad (26)$$

$$\frac{\partial Q}{\partial \boldsymbol{\theta}_j} = -\frac{1}{n} (\boldsymbol{\Psi}_j + \gamma_j \beta_E (X_E \circ \boldsymbol{\Psi}_j))^\top R + \lambda(1 - \alpha) w_j s_2 = \mathbf{0} \quad (27)$$

$$\frac{\partial Q}{\partial \gamma_j} = -\frac{1}{n} (\beta_E (X_E \circ \boldsymbol{\Psi}_j) \boldsymbol{\theta}_j)^\top R + \lambda\alpha w_{jE} s_3 = 0 \quad (28)$$

where s_1 is in the subgradient of the ℓ_1 norm:

$$s_1 \in \begin{cases} \text{sign}(\beta_E) & \text{if } \beta_E \neq 0 \\ [-1, 1] & \text{if } \beta_E = 0, \end{cases}$$

s_2 is in the subgradient of the ℓ_2 norm:

$$s_2 \in \begin{cases} \frac{\boldsymbol{\theta}_j}{\|\boldsymbol{\theta}_j\|_2} & \text{if } \boldsymbol{\theta}_j \neq \mathbf{0} \\ u \in \mathbb{R}^{m_j} : \|u\|_2 \leq 1 & \text{if } \boldsymbol{\theta}_j = \mathbf{0}, \end{cases}$$

B ALGORITHM DETAILS

and s_3 is in the subgradient of the ℓ_1 norm:

$$s_3 \in \begin{cases} \text{sign}(\gamma_j) & \text{if } \gamma_j \neq 0 \\ [-1, 1] & \text{if } \gamma_j = 0. \end{cases}$$

⁶⁶⁸ Define the partial residuals, without the j th predictor for $j = 1, \dots, p$, as

$$R_{(-j)} = Y - \beta_0 \cdot \mathbf{1} - \sum_{\ell \neq j} \Psi_\ell \boldsymbol{\theta}_\ell - \beta_E X_E - \sum_{\ell \neq j} \gamma_\ell \beta_E(X_E \circ \Psi_\ell) \boldsymbol{\theta}_\ell$$

⁶⁶⁹ the partial residual without X_E as

$$R_{(-E)} = Y - \beta_0 \cdot \mathbf{1} - \sum_{j=1}^p \Psi_j \boldsymbol{\theta}_j$$

⁶⁷⁰ and the partial residual without the j th interaction for $j = 1, \dots, p$, as

$$R_{(-jE)} = Y - \beta_0 \cdot \mathbf{1} - \sum_{j=1}^p \Psi_j \boldsymbol{\theta}_j - \beta_E X_E - \sum_{\ell \neq j} \gamma_\ell \beta_E(X_E \circ \Psi_\ell) \boldsymbol{\theta}_\ell$$

From the subgradient equations (25)–(28) we see that

$$\hat{\beta}_0 = \left(Y - \sum_{j=1}^p \Psi_j \hat{\boldsymbol{\theta}}_j - \hat{\beta}_E X_E - \sum_{j=1}^p \hat{\gamma}_j \hat{\beta}_E(X_E \circ \Psi_j) \hat{\boldsymbol{\theta}}_j \right)^\top \mathbf{1} \quad (29)$$

$$\hat{\beta}_E = \frac{S\left(\frac{1}{n \cdot w_E} \left(X_E + \sum_{j=1}^p \hat{\gamma}_j (X_E \circ \Psi_j) \hat{\boldsymbol{\theta}}_j \right)^\top R_{(-E)}, \lambda(1-\alpha) \right)}{\left(X_E + \sum_{j=1}^p \hat{\gamma}_j (X_E \circ \Psi_j) \hat{\boldsymbol{\theta}}_j \right)^\top \left(X_E + \sum_{j=1}^p \hat{\gamma}_j (X_E \circ \Psi_j) \hat{\boldsymbol{\theta}}_j \right)} \quad (30)$$

$$\lambda(1-\alpha) w_j \frac{\boldsymbol{\theta}_j}{\|\boldsymbol{\theta}_j\|_2} = \frac{1}{n} (\Psi_j + \gamma_j \beta_E(X_E \circ \Psi_j))^\top R_{(-j)} \quad (31)$$

$$\hat{\gamma}_j = \frac{S\left(\frac{1}{n \cdot w_{jE}} (\beta_E(X_E \circ \Psi_j) \boldsymbol{\theta}_j)^\top R_{(-jE)}, \lambda\alpha \right)}{(\beta_E(X_E \circ \Psi_j) \boldsymbol{\theta}_j)^\top (\beta_E(X_E \circ \Psi_j) \boldsymbol{\theta}_j)} \quad (32)$$

⁶⁷¹ where $S(x, t) = \text{sign}(x)(|x| - t)$ is the soft-thresholding operator. We see from (29) and (30)

⁶⁷² that there are closed form solutions for the intercept and β_E . From (32), each γ_j also has a

B ALGORITHM DETAILS

closed form solution and can be solved efficiently for $j = 1, \dots, p$ using a coordinate descent procedure [14]. Since there is no closed form solution for β_j , we use a quadratic majorization technique [38] to solve (31). Furthermore, we update each θ_j in a coordinate wise fashion and leverage this to implement further computational speedups which are detailed in Supplemental Section B.2. From these estimates, we compute the interaction effects using the reparametrizations presented in Table 1, e.g., $\hat{\tau}_j = \hat{\gamma}_j \hat{\beta}_E \hat{\theta}_j$, $j = 1, \dots, p$ for the strong heredity **sail** model.

680 B.1 Least-Squares sail with Strong Heredity

681 A more detailed algorithm for fitting the least-squares **sail** model with strong heredity is
682 given in Algorithm 3.

B ALGORITHM DETAILS

Algorithm 3 Blockwise Coordinate Descent for Least-Squares `sail` with Strong Heredity

```

1: function sail( $\mathbf{X}, Y, X_E, \text{basis}, \lambda, \alpha, w_j, w_E, w_{jE}, \epsilon$ )            $\triangleright$  Algorithm for solving (24)
2:    $\Psi_j \leftarrow \text{basis}(X_j)$ ,  $\tilde{\Psi}_j \leftarrow X_E \circ \Psi_j$  for  $j = 1, \dots, p$ 
3:   Initialize:  $\beta_0^{(0)} \leftarrow \bar{Y}$ ,  $\beta_E^{(0)} = \boldsymbol{\theta}_j^{(0)} = \gamma_j^{(0)} \leftarrow 0$  for  $j = 1, \dots, p$ .
4:   Set iteration counter  $k \leftarrow 0$ 
5:    $R^* \leftarrow Y - \beta_0^{(k)} - \beta_E^{(k)} X_E - \sum_j (\Psi_j + \gamma_j^{(k)} \beta_E^{(k)} \tilde{\Psi}_j) \boldsymbol{\theta}_j^{(k)}$ 
6:   repeat
7:     • To update  $\boldsymbol{\gamma} = (\gamma_1, \dots, \gamma_p)$ 
8:        $\tilde{X}_j \leftarrow \beta_E^{(k)} \tilde{\Psi}_j \boldsymbol{\theta}_j^{(k)}$  for  $j = 1, \dots, p$ 
9:        $R \leftarrow R^* + \sum_{j=1}^p \gamma_j^{(k)} \tilde{X}_j$ 
10:      
$$\boldsymbol{\gamma}^{(k)(new)} \leftarrow \arg \min_{\boldsymbol{\gamma}} \frac{1}{2n} \left\| R - \sum_j \gamma_j \tilde{X}_j \right\|_2^2 + \lambda \alpha \sum_j w_{jE} |\gamma_j|$$

11:       $\Delta = \sum_j (\gamma_j^{(k)} - \gamma_j^{(k)(new)}) \tilde{X}_j$ 
12:       $R^* \leftarrow R^* + \Delta$ 
13:      • To update  $\boldsymbol{\theta} = (\boldsymbol{\theta}_1, \dots, \boldsymbol{\theta}_p)$ 
14:         $\tilde{X}_j \leftarrow \Psi_j + \gamma_j^{(k)} \beta_E^{(k)} \tilde{\Psi}_j$  for  $j = 1, \dots, p$ 
15:        for  $j = 1, \dots, p$  do
16:           $R \leftarrow R^* + \tilde{X}_j \boldsymbol{\theta}_j^{(k)}$ 
17:          
$$\boldsymbol{\theta}_j^{(k)(new)} \leftarrow \arg \min_{\boldsymbol{\theta}_j} \frac{1}{2n} \left\| R - \tilde{X}_j \boldsymbol{\theta}_j \right\|_2^2 + \lambda(1 - \alpha) w_j \|\boldsymbol{\theta}_j\|_2$$

18:           $\Delta = \tilde{X}_j (\boldsymbol{\theta}_j^{(k)} - \boldsymbol{\theta}_j^{(k)(new)})$ 
19:           $R^* \leftarrow R^* + \Delta$ 
20:          • To update  $\beta_E$ 
21:             $\tilde{X}_E \leftarrow X_E + \sum_j \gamma_j^{(k)} \tilde{\Psi}_j \boldsymbol{\theta}_j^{(k)}$ 
22:             $R \leftarrow R^* + \beta_E^{(k)} \tilde{X}_E$ 
23:            
$$\beta_E^{(k)(new)} \leftarrow \frac{1}{\tilde{X}_E^\top \tilde{X}_E} S \left( \frac{1}{n \cdot w_E} \tilde{X}_E^\top R, \lambda(1 - \alpha) \right)$$

24:            
$$\Delta = (\beta_E^{(k)} - \beta_E^{(k)(new)}) \tilde{X}_E$$

25:             $R^* \leftarrow R^* + \Delta$ 
26:            • To update  $\beta_0$ 
27:               $R \leftarrow R^* + \beta_0^{(k)}$ 
28:              
$$\beta_0^{(k)(new)} \leftarrow \frac{1}{n} R^* \cdot \mathbf{1}$$

29:               $\Delta = \beta_0^{(k)} - \beta_0^{(k)(new)}$ 
30:               $R^* \leftarrow R^* + \Delta$ 
31:               $k \leftarrow k + 1$ 
32:            until convergence criterion is satisfied:  $|Q(\Phi^{(k-1)}) - Q(\Phi^{(k)})| / Q(\Phi^{(k-1)}) < \epsilon$ 

```

B ALGORITHM DETAILS

683 B.2 Details on Update for θ

Here we discuss a computational speedup in the updates for the θ parameter. The partial residual (R_s) used for updating θ_s ($s \in 1, \dots, p$) at the k th iteration is given by

$$R_s = Y - \tilde{Y}_{(-s)}^{(k)} \quad (33)$$

where $\tilde{Y}_{(-s)}^{(k)}$ is the fitted value at the k th iteration excluding the contribution from Ψ_s :

$$\tilde{Y}_{(-s)}^{(k)} = \beta_0^{(k)} - \beta_E^{(k)} X_E - \sum_{\ell \neq s} \Psi_\ell \theta_\ell^{(k)} - \sum_{\ell \neq s} \gamma_\ell^{(k)} \beta_E^{(k)} \tilde{\Psi}_\ell \theta_\ell^{(k)} \quad (34)$$

Using (34), (33) can be re-written as

$$\begin{aligned} R_s &= Y - \beta_0^{(k)} - \beta_E^{(k)} X_E - \sum_{j=1}^p (\Psi_j + \gamma_j^{(k)} \beta_E^{(k)} \tilde{\Psi}_j) \theta_j^{(k)} + (\Psi_s + \gamma_s^{(k)} \beta_E^{(k)} \tilde{\Psi}_s) \theta_s^{(k)} \\ &= R^* + (\Psi_s + \gamma_s^{(k)} \beta_E^{(k)} \tilde{\Psi}_s) \theta_s^{(k)} \end{aligned} \quad (35)$$

684 where

$$R^* = Y - \beta_0^{(k)} - \beta_E^{(k)} X_E - \sum_{j=1}^p (\Psi_j + \gamma_j^{(k)} \beta_E^{(k)} \tilde{\Psi}_j) \theta_j^{(k)} \quad (36)$$

Denote $\theta_s^{(k)(new)}$ the solution for predictor s at the k th iteration, given by:

$$\theta_s^{(k)(new)} = \arg \min_{\theta_j} \frac{1}{2n} \left\| R_s - (\Psi_s + \gamma_s^{(k)} \beta_E^{(k)} \tilde{\Psi}_s) \theta_j \right\|_2^2 + \lambda(1-\alpha) w_s \|\theta_j\|_2 \quad (37)$$

Now we want to update the parameters for the next predictor θ_{s+1} ($s+1 \in 1, \dots, p$) at the k th iteration. The partial residual used to update θ_{s+1} is given by

$$R_{s+1} = R^* + (\Psi_{s+1} + \gamma_{s+1}^{(k)} \beta_E^{(k)} \tilde{\Psi}_{s+1}) \theta_{s+1}^{(k)} + (\Psi_s + \gamma_s^{(k)} \beta_E^{(k)} \tilde{\Psi}_s) (\theta_s^{(k)} - \theta_s^{(k)(new)}) \quad (38)$$

B ALGORITHM DETAILS

where R^* is given by (36), $\boldsymbol{\theta}_s^{(k)}$ is the parameter value prior to the update, and $\boldsymbol{\theta}_s^{(k)(new)}$ is the updated value given by (37). Taking the difference between (35) and (38) gives

$$\begin{aligned}\Delta &= R_t - R_s \\ &= (\Psi_t + \gamma_t^{(k)} \beta_E^{(k)} \tilde{\Psi}_t) \boldsymbol{\theta}_t^{(k)} + (\Psi_s + \gamma_s^{(k)} \beta_E^{(k)} \tilde{\Psi}_s) (\boldsymbol{\theta}_s^{(k)} - \boldsymbol{\theta}_s^{(k)(new)}) - (\Psi_s + \gamma_s^{(k)} \beta_E^{(k)} \tilde{\Psi}_s) \boldsymbol{\theta}_s^{(k)} \\ &= (\Psi_t + \gamma_t^{(k)} \beta_E^{(k)} \tilde{\Psi}_t) \boldsymbol{\theta}_t^{(k)} - (\Psi_s + \gamma_s^{(k)} \beta_E^{(k)} \tilde{\Psi}_s) \boldsymbol{\theta}_s^{(k)(new)}\end{aligned}\quad (39)$$

685 Therefore $R_t = R_s + \Delta$, and the partial residual for updating the next predictor can be
 686 computed by updating the previous partial residual by Δ , given by (39). This formulation
 687 can lead to computational speedups especially when $\Delta = 0$, meaning the partial residual
 688 does not need to be re-calculated.

689 B.3 Maximum penalty parameter (λ_{max}) for strong heredity

690 The subgradient equations (26)–(28) can be used to determine the largest value of λ such
 691 that all coefficients are 0. From the subgradient Equation (26), we see that $\beta_E = 0$ is a
 692 solution if

$$\frac{1}{w_E} \left| \frac{1}{n} \left(X_E + \sum_{j=1}^p \gamma_j (X_E \circ \Psi_j) \boldsymbol{\theta}_j \right)^\top R_{(-E)} \right| \leq \lambda(1 - \alpha) \quad (40)$$

693 From the subgradient Equation (27), we see that $\boldsymbol{\theta}_j = \mathbf{0}$ is a solution if

$$\frac{1}{w_j} \left\| \frac{1}{n} (\Psi_j + \gamma_j \beta_E (X_E \circ \Psi_j))^\top R_{(-j)} \right\|_2 \leq \lambda(1 - \alpha) \quad (41)$$

694 From the subgradient Equation (28), we see that $\gamma_j = 0$ is a solution if

$$\frac{1}{w_{jE}} \left| \frac{1}{n} (\beta_E (X_E \circ \Psi_j) \boldsymbol{\theta}_j)^\top R_{(-jE)} \right| \leq \lambda\alpha \quad (42)$$

B ALGORITHM DETAILS

Due to the strong heredity property, the parameter vector $(\beta_E, \boldsymbol{\theta}_1, \dots, \boldsymbol{\theta}_p, \gamma_1, \dots, \gamma_p)$ will be entirely equal to $\mathbf{0}$ if $(\beta_E, \boldsymbol{\theta}_1, \dots, \boldsymbol{\theta}_p) = \mathbf{0}$. Therefore, the smallest value of λ for which the entire parameter vector (excluding the intercept) is $\mathbf{0}$ is:

$$\lambda_{max} = \frac{1}{n(1-\alpha)} \max \left\{ \frac{1}{w_E} \left(X_E + \sum_{j=1}^p \gamma_j (X_E \circ \boldsymbol{\Psi}_j) \boldsymbol{\theta}_j \right)^\top R_{(-E)}, \right. \\ \left. \max_j \frac{1}{w_j} \left\| (\boldsymbol{\Psi}_j + \gamma_j \beta_E (X_E \circ \boldsymbol{\Psi}_j))^\top R_{(-j)} \right\|_2 \right\} \quad (43)$$

which reduces to

$$\lambda_{max} = \frac{1}{n(1-\alpha)} \max \left\{ \frac{1}{w_E} (X_E)^\top R_{(-E)}, \max_j \frac{1}{w_j} \left\| (\boldsymbol{\Psi}_j)^\top R_{(-j)} \right\|_2 \right\}$$

⁶⁹⁵ B.4 Least-Squares sail with Weak Heredity

⁶⁹⁶ The least-squares sail model with weak heredity has the form

$$\hat{Y} = \beta_0 \cdot \mathbf{1} + \sum_{j=1}^p \boldsymbol{\Psi}_j \boldsymbol{\theta}_j + \beta_E X_E + \sum_{j=1}^p \gamma_j (X_E \circ \boldsymbol{\Psi}_j) (\beta_E \cdot \mathbf{1}_{m_j} + \boldsymbol{\theta}_j) \quad (44)$$

⁶⁹⁷ The objective function is given by

$$Q(\boldsymbol{\Phi}) = \frac{1}{2n} \left\| Y - \hat{Y} \right\|_2^2 + \lambda(1-\alpha) \left(w_E |\beta_E| + \sum_{j=1}^p w_j \|\boldsymbol{\theta}_j\|_2 \right) + \lambda \alpha \sum_{j=1}^p w_{jE} |\gamma_j| \quad (45)$$

B ALGORITHM DETAILS

Denote the n -dimensional residual column vector $R = Y - \hat{Y}$. The subgradient equations are given by

$$\frac{\partial Q}{\partial \beta_0} = \frac{1}{n} \left(Y - \beta_0 \cdot \mathbf{1} - \sum_{j=1}^p \Psi_j \boldsymbol{\theta}_j - \beta_E X_E - \sum_{j=1}^p \gamma_j (X_E \circ \Psi_j) (\beta_E \cdot \mathbf{1}_{m_j} + \boldsymbol{\theta}_j) \right)^\top \mathbf{1} = 0 \quad (46)$$

$$\frac{\partial Q}{\partial \beta_E} = -\frac{1}{n} \left(X_E + \sum_{j=1}^p \gamma_j (X_E \circ \Psi_j) \mathbf{1}_{m_j} \right)^\top R + \lambda(1-\alpha) w_E s_1 = 0 \quad (47)$$

$$\frac{\partial Q}{\partial \boldsymbol{\theta}_j} = -\frac{1}{n} (\Psi_j + \gamma_j (X_E \circ \Psi_j))^\top R + \lambda(1-\alpha) w_j s_2 = \mathbf{0} \quad (48)$$

$$\frac{\partial Q}{\partial \gamma_j} = -\frac{1}{n} ((X_E \circ \Psi_j) (\beta_E \cdot \mathbf{1}_{m_j} + \boldsymbol{\theta}_j))^\top R + \lambda \alpha w_{jE} s_3 = 0 \quad (49)$$

where s_1 is in the subgradient of the ℓ_1 norm:

$$s_1 \in \begin{cases} \text{sign}(\beta_E) & \text{if } \beta_E \neq 0 \\ [-1, 1] & \text{if } \beta_E = 0, \end{cases}$$

s_2 is in the subgradient of the ℓ_2 norm:

$$s_2 \in \begin{cases} \frac{\boldsymbol{\theta}_j}{\|\boldsymbol{\theta}_j\|_2} & \text{if } \boldsymbol{\theta}_j \neq \mathbf{0} \\ u \in \mathbb{R}^{m_j} : \|u\|_2 \leq 1 & \text{if } \boldsymbol{\theta}_j = \mathbf{0}, \end{cases}$$

and s_3 is in the subgradient of the ℓ_1 norm:

$$s_3 \in \begin{cases} \text{sign}(\gamma_j) & \text{if } \gamma_j \neq 0 \\ [-1, 1] & \text{if } \gamma_j = 0. \end{cases}$$

698 Define the partial residuals, without the j th predictor for $j = 1, \dots, p$, as

$$R_{(-j)} = Y - \beta_0 \cdot \mathbf{1} - \sum_{\ell \neq j} \Psi_\ell \boldsymbol{\theta}_\ell - \beta_E X_E - \sum_{\ell \neq j} \gamma_\ell (X_E \circ \Psi_\ell) (\beta_E \cdot \mathbf{1}_{m_\ell} + \boldsymbol{\theta}_\ell)$$

B ALGORITHM DETAILS

⁶⁹⁹ the partial residual without X_E as

$$R_{(-E)} = Y - \beta_0 \cdot \mathbf{1} - \sum_{j=1}^p \Psi_j \boldsymbol{\theta}_j - \sum_{j=1}^p \gamma_j (X_E \circ \Psi_j) \boldsymbol{\theta}_j$$

⁷⁰⁰ and the partial residual without the j th interaction for $j = 1, \dots, p$

$$R_{(-jE)} = Y - \beta_0 \cdot \mathbf{1} - \sum_{j=1}^p \Psi_j \boldsymbol{\theta}_j - \beta_E X_E - \sum_{\ell \neq j} \gamma_\ell (X_E \circ \Psi_\ell) (\beta_E \cdot \mathbf{1}_{m_\ell} + \boldsymbol{\theta}_\ell)$$

⁷⁰¹ From the subgradient Equation (47), we see that $\beta_E = 0$ is a solution if

$$\frac{1}{w_E} \left| \frac{1}{n} \left(X_E + \sum_{j=1}^p \gamma_j (X_E \circ \Psi_j) \mathbf{1}_{m_j} \right)^\top R_{(-E)} \right| \leq \lambda(1-\alpha) \quad (50)$$

⁷⁰² From the subgradient Equation (48), we see that $\boldsymbol{\theta}_j = \mathbf{0}$ is a solution if

$$\frac{1}{w_j} \left\| \frac{1}{n} (\Psi_j + \gamma_j (X_E \circ \Psi_j))^\top R_{(-j)} \right\|_2 \leq \lambda(1-\alpha) \quad (51)$$

⁷⁰³ From the subgradient Equation (49), we see that $\gamma_j = 0$ is a solution if

$$\frac{1}{w_{jE}} \left| \frac{1}{n} ((X_E \circ \Psi_j) (\beta_E \cdot \mathbf{1}_{m_j} + \boldsymbol{\theta}_j))^\top R_{(-jE)} \right| \leq \lambda\alpha \quad (52)$$

B ALGORITHM DETAILS

From the subgradient equations we see that

$$\hat{\beta}_0 = \left(Y - \sum_{j=1}^p \boldsymbol{\Psi}_j \hat{\boldsymbol{\theta}}_j - \hat{\beta}_E X_E - \sum_{j=1}^p \hat{\gamma}_j (X_E \circ \boldsymbol{\Psi}_j) (\hat{\beta}_E \cdot \mathbf{1}_{m_j} + \hat{\boldsymbol{\theta}}_j) \right)^\top \mathbf{1} \quad (53)$$

$$\hat{\beta}_E = \frac{S \left(\frac{1}{n \cdot w_E} \left(X_E + \sum_{j=1}^p \hat{\gamma}_j (X_E \circ \boldsymbol{\Psi}_j) \mathbf{1}_{m_j} \right)^\top R_{(-E)}, \lambda(1-\alpha) \right)}{\left(X_E + \sum_{j=1}^p \hat{\gamma}_j (X_E \circ \boldsymbol{\Psi}_j) \mathbf{1}_{m_j} \right)^\top \left(X_E + \sum_{j=1}^p \hat{\gamma}_j (X_E \circ \boldsymbol{\Psi}_j) \mathbf{1}_{m_j} \right)} \quad (54)$$

$$\lambda(1-\alpha) w_j \frac{\boldsymbol{\theta}_j}{\|\boldsymbol{\theta}_j\|_2} = \frac{1}{n} (\boldsymbol{\Psi}_j + \gamma_j (X_E \circ \boldsymbol{\Psi}_j))^\top R_{(-j)} \quad (55)$$

$$\hat{\gamma}_j = \frac{S \left(\frac{1}{n \cdot w_{jE}} \left((X_E \circ \boldsymbol{\Psi}_j) (\beta_E \cdot \mathbf{1}_{m_j} + \boldsymbol{\theta}_j) \right)^\top R_{(-jE)}, \lambda \alpha \right)}{\left((X_E \circ \boldsymbol{\Psi}_j) (\beta_E \cdot \mathbf{1}_{m_j} + \boldsymbol{\theta}_j) \right)^\top \left((X_E \circ \boldsymbol{\Psi}_j) (\beta_E \cdot \mathbf{1}_{m_j} + \boldsymbol{\theta}_j) \right)} \quad (56)$$

where $S(x, t) = \text{sign}(x)(|x|-t)$ is the soft-thresholding operator. As was the case in the strong heredity **sail** model, there are closed form solutions for the intercept and β_E , each γ_j also has a closed form solution and can be solved efficiently for $j = 1, \dots, p$ using the coordinate descent procedure implemented in the **glmnet** package [14], while we use the quadratic majorization technique implemented in the **gglasso** package [38] to solve (55). Algorithm 4 details the procedure used to fit the least-squares weak heredity **sail** model.

710 B.4.1 Maximum penalty parameter (λ_{max}) for weak heredity

711 The smallest value of λ for which the entire parameter vector $(\beta_E, \boldsymbol{\theta}_1, \dots, \boldsymbol{\theta}_p, \gamma_1, \dots, \gamma_p)$ is **0**
712 is:

$$\begin{aligned} \lambda_{max} = & \frac{1}{n} \max \left\{ \frac{1}{(1-\alpha)w_E} \left(X_E + \sum_{j=1}^p \gamma_j (X_E \circ \boldsymbol{\Psi}_j) \mathbf{1}_{m_j} \right)^\top R_{(-E)}, \right. \\ & \max_j \frac{1}{(1-\alpha)w_j} \left\| (\boldsymbol{\Psi}_j + \gamma_j (X_E \circ \boldsymbol{\Psi}_j))^\top R_{(-j)} \right\|_2, \\ & \left. \max_j \frac{1}{\alpha w_{jE}} \left((X_E \circ \boldsymbol{\Psi}_j) (\beta_E \cdot \mathbf{1}_{m_j} + \boldsymbol{\theta}_j) \right)^\top R_{(-jE)} \right\} \quad (57) \end{aligned}$$

B ALGORITHM DETAILS

Algorithm 4 Coordinate descent for least-squares sail with weak heredity

```

1: function sail( $X, Y, X_E, \text{basis}, \lambda, \alpha, w_j, w_E, w_{jE}, \epsilon$ )            $\triangleright$  Algorithm for solving (45)
2:    $\Psi_j \leftarrow \text{basis}(X_j)$ ,  $\tilde{\Psi}_j \leftarrow X_E \circ \Psi_j$  for  $j = 1, \dots, p$ 
3:   Initialize:  $\beta_0^{(0)} \leftarrow \bar{Y}$ ,  $\beta_E^{(0)} = \boldsymbol{\theta}_j^{(0)} = \gamma_j^{(0)} \leftarrow 0$  for  $j = 1, \dots, p$ .
4:   Set iteration counter  $k \leftarrow 0$ 
5:    $R^* \leftarrow Y - \beta_0^{(k)} - \beta_E^{(k)} X_E - \sum_j \Psi_j \boldsymbol{\theta}_j^{(k)} - \sum_j \gamma_j^{(k)} \tilde{\Psi}_j (\beta_E^{(k)} \cdot \mathbf{1}_{m_j} + \boldsymbol{\theta}_j^{(k)})$ 
6:   repeat
7:     • To update  $\boldsymbol{\gamma} = (\gamma_1, \dots, \gamma_p)$ 
8:        $\tilde{X}_j \leftarrow \tilde{\Psi}_j (\beta_E^{(k)} \cdot \mathbf{1}_{m_j} + \boldsymbol{\theta}_j^{(k)})$       for  $j = 1, \dots, p$ 
9:        $R \leftarrow R^* + \sum_{j=1}^p \gamma_j^{(k)} \tilde{X}_j$ 
10:      
$$\boldsymbol{\gamma}^{(k)(new)} \leftarrow \arg \min_{\boldsymbol{\gamma}} \frac{1}{2n} \left\| R - \sum_j \gamma_j \tilde{X}_j \right\|_2^2 + \lambda \alpha \sum_j w_{jE} |\gamma_j|$$

11:       $\Delta = \sum_j (\gamma_j^{(k)} - \gamma_j^{(k)(new)}) \tilde{X}_j$ 
12:       $R^* \leftarrow R^* + \Delta$ 
13:      • To update  $\boldsymbol{\theta} = (\boldsymbol{\theta}_1, \dots, \boldsymbol{\theta}_p)$ 
14:         $\tilde{X}_j \leftarrow \Psi_j + \gamma_j^{(k)} \tilde{\Psi}_j$  for  $j = 1, \dots, p$ 
15:        for  $j = 1, \dots, p$  do
16:           $R \leftarrow R^* + \tilde{X}_j \boldsymbol{\theta}_j^{(k)}$ 
17:          
$$\boldsymbol{\theta}_j^{(k)(new)} \leftarrow \arg \min_{\boldsymbol{\theta}_j} \frac{1}{2n} \left\| R - \tilde{X}_j \boldsymbol{\theta}_j \right\|_2^2 + \lambda(1 - \alpha) w_j \|\boldsymbol{\theta}_j\|_2$$

18:           $\Delta = \tilde{X}_j (\boldsymbol{\theta}_j^{(k)} - \boldsymbol{\theta}_j^{(k)(new)})$ 
19:           $R^* \leftarrow R^* + \Delta$ 
20:          • To update  $\beta_E$ 
21:             $\tilde{X}_E \leftarrow X_E + \sum_j \gamma_j^{(k)} \tilde{\Psi}_j \mathbf{1}_{m_j}$ 
22:             $R \leftarrow R^* + \beta_E^{(k)} \tilde{X}_E$ 
23:            
$$\beta_E^{(k)(new)} \leftarrow \frac{1}{\tilde{X}_E^\top \tilde{X}_E} S \left( \frac{1}{n \cdot w_E} \tilde{X}_E^\top R, \lambda(1 - \alpha) \right)$$

24:            
$$\triangleright S(x, t) = \text{sign}(x)(|x| - t)_+$$

25:             $\Delta = (\beta_E^{(k)} - \beta_E^{(k)(new)}) \tilde{X}_E$ 
26:             $R^* \leftarrow R^* + \Delta$ 
27:            • To update  $\beta_0$ 
28:               $R \leftarrow R^* + \beta_0^{(k)}$ 
29:              
$$\beta_0^{(k)(new)} \leftarrow \frac{1}{n} R^* \cdot \mathbf{1}$$

30:               $\Delta = \beta_0^{(k)} - \beta_0^{(k)(new)}$ 
31:               $R^* \leftarrow R^* + \Delta$ 
32:               $k \leftarrow k + 1$ 
33:              until convergence criterion is satisfied:  $|Q(\Phi^{(k-1)}) - Q(\Phi^{(k)})| / Q(\Phi^{(k-1)}) < \epsilon$ 

```

C ADDITIONAL RESULTS ON PRS FOR EDUCATIONAL ATTAINMENT

which reduces to

$$\lambda_{max} = \frac{1}{n(1-\alpha)} \max \left\{ \frac{1}{w_E} (X_E)^\top R_{(-E)}, \max_j \frac{1}{w_j} \|(\Psi_j)^\top R_{(-j)}\|_2 \right\}$$

⁷¹³ This is the same λ_{max} as the least-squares strong heredity **sail** model.

⁷¹⁴ C Additional Results on PRS for Educational Attainment

⁷¹⁵

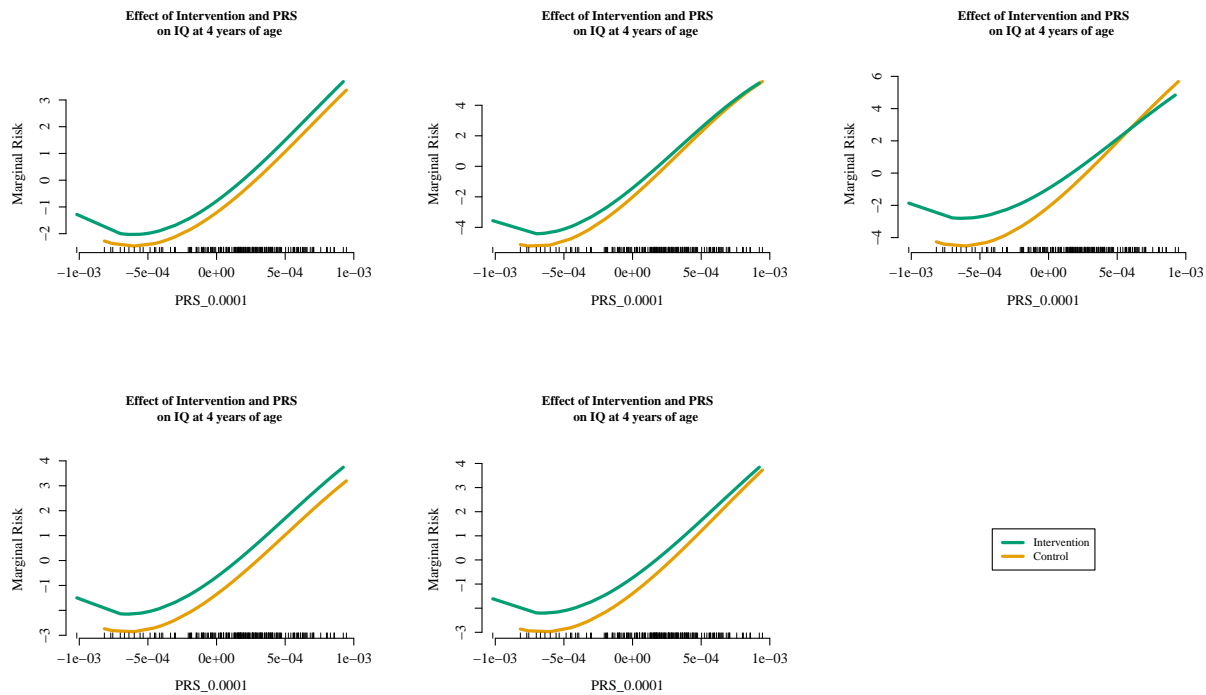


Figure C.1: Estimated interaction effect identified by the weak heredity **sail** using cubic B-splines and $\alpha = 0.1$ for the Nurse Family Partnership data for the 5 imputed datasets. Of the 189 subjects, 19 IQ scores were imputed using **mice** [5]. The selected model, chosen via 10-fold cross-validation, contained three variables: the main effects for the intervention and the PRS for educational attainment using genetic variants significant at the 0.0001 level, as well as their interaction.

C ADDITIONAL RESULTS ON PRS FOR EDUCATIONAL ATTAINMENT

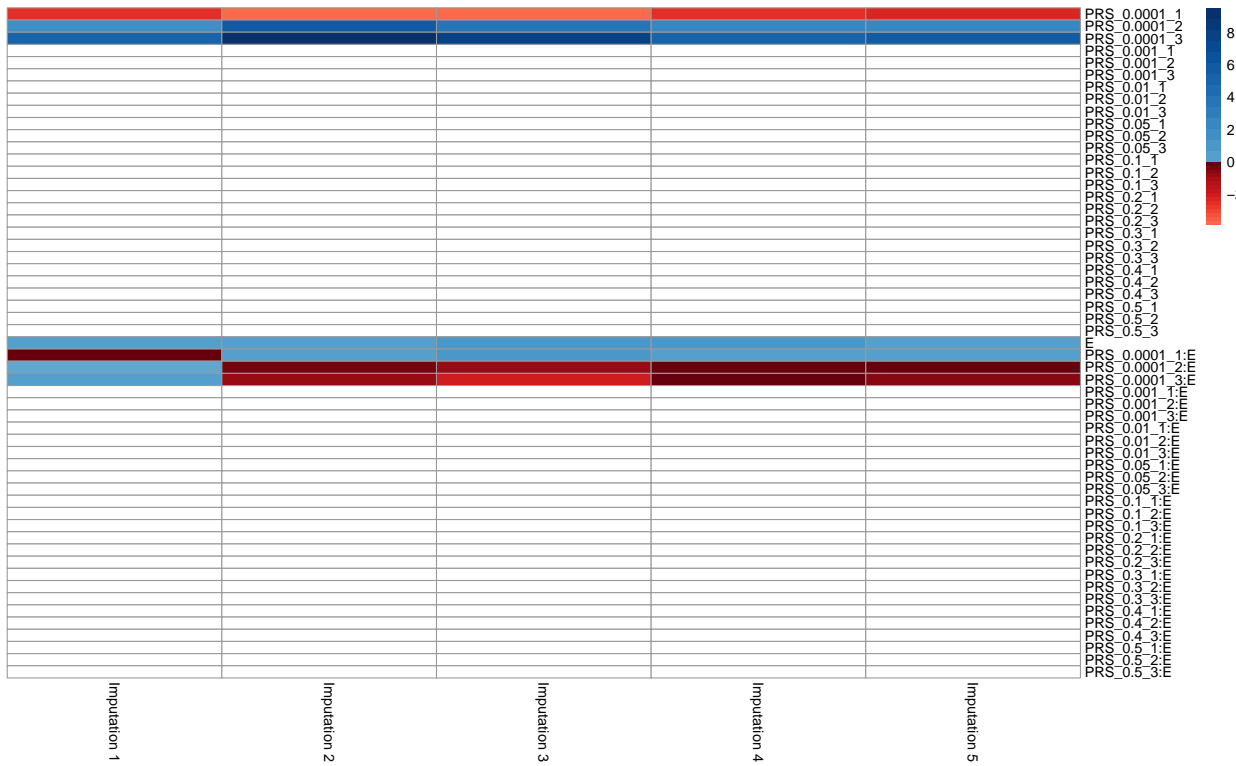


Figure C.2: Coefficient estimates obtained by the weak heredity `sail` using cubic B-splines and $\alpha = 0.1$ for the Nurse Family Partnership data for the 5 imputed datasets. Of the 189 subjects, 19 IQ scores were imputed using `mice` [5]. The selected model, chosen via 10-fold cross-validation, contained three variables: the main effects for the intervention and the PRS for educational attainment using genetic variants significant at the 0.0001 level, as well as their interaction. This results was consistent across all 5 imputed datasets. The white boxes indicate a coefficient estimate of 0.